DEVELOPMENT OF ICE RELEASING EPOXY-SILOXANE MARINE COATINGS

A Thesis
Submitted to the Graduate Faculty
of the
North Dakota State University
of Agriculture and Applied Science

By

Morgen James Hagerott

In Partial Fulfillment of the Requirements
for the Degree of
MASTER OF SCIENCE

Major Department:
Coatings and Polymeric Materials

May 2022

Fargo, North Dakota

North Dakota State University
Graduate School

Title

Development of Ice Releasing Epoxy-Siloxane Marine Coatings

By

Morgen Hagerott

The Supervisory Committee certifies that this ***disquisition*** complies with North Dakota State University's regulations and meets the accepted standards for the degree of

MASTER OF SCIENCE

SUPERVISORY COMMITTEE:

Dr. Dean C. Webster
Chair

Dr. Mohiuddin Quadir

Dr. Jessica Vold

Approved:

7-7-2022
Date

Dr. Dean Webster
Department Chair

ABSTRACT

In this study, epoxy-siloxane coatings were prepared and modified using various polysiloxane oil additives with the goal of developing an ice releasing epoxy-siloxane coating. Contact angle, surface energy, and ice adhesion tests were conducted to study the effect each oil additive had on the surface properties of the coatings. Additionally, antifouling and fouling release properties were assessed using two micro-organisms, *Cellulophaga lytica* and *Navicula incerta,* and one macro-organism, *Amphibalanus Amphitrite* (barnacles). The goal of which was to compare the ice and fouling releasing properties of the coatings to see if any correlations could be made between the two. One of the coating formulations yielded lower ice adhesion and barnacle adhesion. The 5% PMDM-010s, coating with oil containing 8-12% phenylmethylsiloxane and 88-92% dimethylsiloxane, showed improved properties compared to the base coating and outperformed the other coating formulations that containing oils of different composition.

ACKNOWLEDGMENTS

Firstly, I would like to thank my advisor Dr. Dean Webster for his guidance throughout my time in the Coatings and Polymeric Materials department. To my committee members, Dr. Jessica Vold and Dr. Mohiuddin Quadir, I thank you for taking the time to sit on my committee providing comments and advice.

I would also like to thank Shane Stafslien and lyndsi Vanderwal for their assistance with all the biological assays conducted for this research. Thank you to Dr. Dev Gurera and Dr. Anish Tuteja for their collaboration on ice releasing testing. Thank you to Jim Bahr and Dr. Chunju Gu for helping with instrumentation and characterization throughout the entire lab. To the CPM faculty and classmates, thank you for making every day in the lab enjoyable. I truly appreciate all of you for the experience and knowledge that you shared with me.

To my parents, David and Dawn, I cannot thank you enough for your support throughout my entire life. From a very young age you instilled in me the importance of my education. To my girlfriend Erica Solberg, thank you for your unending encouragement throughout college. Thank you for motivating me to constantly reach higher and to do my absolute best in everything that I do in life.

I would also like to thank the Office of Naval Research for providing the funding for the project that I worked on. Lastly, I would like to thank North Dakota State University. The place that I have spent the last four years learning and creating memories that I will cherish forever.

DEDICATION

I would like to dedicate this thesis to my family, David, Dawn, and Gabe, and to my girlfriend Erica. Your constant encouragement, support, and guidance brought me to where I am today.

TABLE OF CONTENTS

LIST OF TABLES

LIST OF FIGURES

CHAPTER 1. INTRODUCTION

Ice Accretion - Overview, Mechanism, and Mitigation Methods

The accretion of ice on a surface that is exposed to freezing conditions affects a variety of infrastructure such as aircraft, power cables, wind/solar power, and ships.[1-7] It occurs due to freezing precipitation or supercooled moisture in the air. Ice accretion, due to supercooled moisture in the air, often occurs on aircraft and can pose a serious risk to safety.[2,3] Two main methods to mitigate ice accretion are anti-icing and deicing techniques. The term anti-icing refers to methods that attempt to prevent the accretion of ice. Whereas deicing refers to the removal of ice, either actively or passively utilizing ice releasing materials. Chemical anti-icing and deicing methods are commonly used on aircraft. When it is expected that an aircraft will encounter below freezing temperatures, a chemical deicer will be sprayed before each flight.[8] Deicing chemicals are also often used after a flight in which an aircraft has accumulated ice. While this approach is effective, the chemicals used can negatively impact the environment.[9-11] Trace amounts of the deicing and anti-icing chemicals have been found in the snow and runoff surrounding airports.[11,13] Natural deicing chemicals are being developed to limit this undesirable impact on the environment.[12]

Ice accretion is widely prevalent and can have serious consequences if steps are not taken to mitigate or remove it. Anti-icing coatings are not currently a dependable method to stop ice accretion. Because of this, costly and potentially harmful chemical substances are used to efficiently remove ice. Therefore, ice releasing surfaces are being researched to remove ice in a manner that is efficient, cost effective, and does not harm the environment.

Ice Accretion Processes - Conditions, Modeling, and Measurement Methods

In order to design new materials and coatings that limit or prevent the accretion of ice, it is important to understand how and where this ice accretes. This process heavily depends on the object that the ice is forming on, and the conditions present. Ice accretion will occur much differently on an aircraft or wind turbine blade than solar panels or power cables.[4,14-16] Temperature is also a significant factor in the formation of ice, specifically the type of ice. When a droplet impacts an object, the ability of that droplet to dissipate heat determines how it freezes onto the surface. The two main types of ice accretion are rime icing and glaze icing.[1,30-32] At lower temperatures, rime icing generally occurs. Due to the low temperature, a supercooled droplet instantly turns into ice upon impact with a surface.[30] In contrast, glaze icing occurs at warmer temperatures.[30] Upon impact, the water does not freeze instantly and is able to flow freely for a short time.[30] Because of this, glaze and rime ice will have a different effect on the object the ice is accreting on.[30-32]

Ice Accretion of Airfoils

At low temperatures, supercooled droplets suspended in clouds can impact an aircraft, causing the droplets to freeze onto the aircraft.[21] Depending on the temperature, size, and volume of the droplets, water can spread down the aircraft and begin accumulating at significant levels. Due to the complexity of ice accretion on aircraft, multiple variables need to be considered to accurately model it.[22] Several studies have been conducted modeling the effects of ice accretion on aircraft and flight dynamics.[5,21-24] Mingione et al. have simulated the impact of supercooled fluid on both single and multi-element airfoils. In this study, both aerodynamic and thermodynamic models were analyzed and compared to experimental data.[21] The study laid out a three-part simulation to properly model the ice accretion: calculation of airflow around the

aircraft, water droplet trajectories based on angle of impact and volume of water, and the heat transfer coefficient.[21] Ice accretion on aircraft wings can have a dangerous effect on the lift, potentially leading to aircraft failure.[5] Mingione et al. used theoretical predictions and simulations to compare to the experimental results gathered from a previous study done by Shin and Bond. In this study, air temperature, liquid water content (LWC), and spray time were tested for repeatability.[25] These tests were conducted using the NASA Lewis Icing Research Tunnel (IRT) (Figure 1.1).

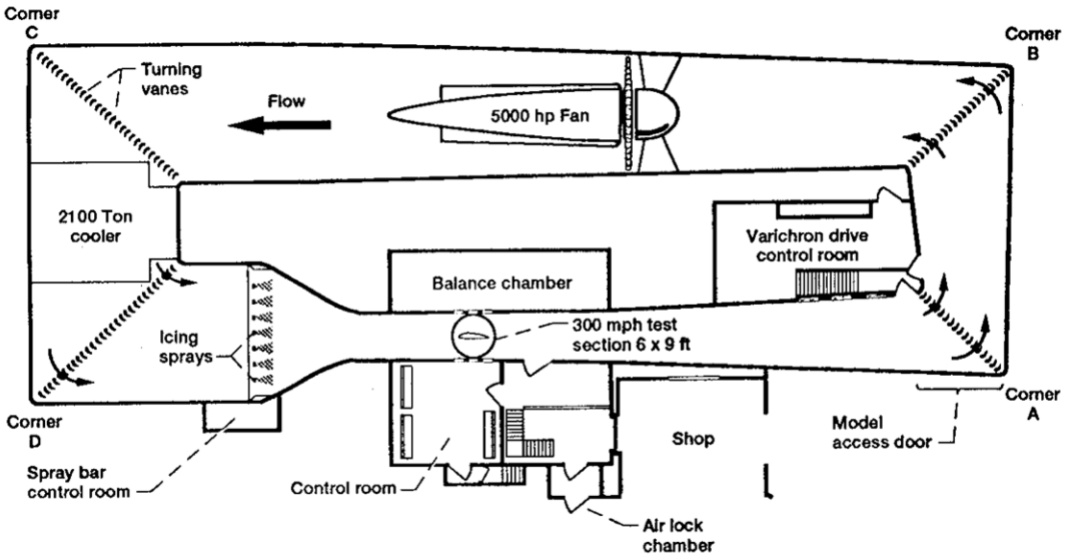

Figure 1.1. Schematic of the NASA Lewis Icing Research Tunnel used to conduct ice accretion experiments. Reprinted from reference 25.

Mingione et al. used the results from this experimental study and compared the data to the predictions that were developed to evaluate the accuracy and reliability of these predictions. The experimental data obtained was compared to the predictor-corrector model and the multi-time-step model.[21] It was determined that for lower air temperatures, where rime ice forms, both the predictor-corrector and multi-time-step model were sufficient. At higher air temperatures, where glaze ice is formed, the multi-time-step model is closer to the experimental measurements done.[21,25] Additionally, the impact of droplets on a multi-element airfoil was investigated. This

heavily relied on angle of impact and viscosity of the fluid.[25,26] The studied concluded that droplets having larger median volumetric diameter and liquid water content typically lead to more ice accretion. Even so, other environmental factors can produce a different outcome.[21]

Figure 1.2. Impact angle of droplet on two-element airfoil (*left):* 0° (*right):* 8.1°. Reprinted from reference 25.

Makkonen et al. used the experimental data from Shin and Bond and compared the results to the TURBICE modeling of ice accretion on wind turbine blades. Predicition of wind turbine icing is more difficult due to multiple potential angles of droplet impact.[4,20] Even with the additional variables present for turbine blades vs aircraft, the TURBICE model was able to accurately replicate the experimental data collected using the Lewis IRT. Another approach was using the TURBICE prediction model to better utilize heating mechanisms within the blades as an ice prevention method. Knowing where droplets most frequetly impact, allows for targeted heating mechanisms that maximize efficiency.[4] This is typically done using sensors that can detect when ice is present, and when a large amount of ice has accumulated.[27] Li et al. conducted a study in which an airfoil was exposed to water spray at a multitude of angles in both a static and rotating state.[28] The airfoils that were rotated had an even layer of ice across the entire surface, whereas the static airfoils had localized ice accretion on the side exposed to the wind spray, similar to aircraft.[25, 28] This is a good indication of how icing will occur, but with the

rotation of the blades and the wind coming from different directions, it is difficult to repeatibly predict how the ice will accrete on a wind turbine blade.[25,28]

Ice Accretion of Power Lines

Power lines, like wind turbine blades, are exposed to droplets in the form of precipitation and wind. Fu et al. studied the accretion of ice on power lines in which they modeled the ice accretion of a cylindrical shape exposed to icing conditions, and found that ice accretion was dependent on cable diameter.[16] Cables of smaller diameter had a faster rate of ice accretion, while larger cables accreted more ice mass.[16] However, this study did not account for the rotation that occurs to power lines as ice accretion changes the weight distribution.[16] Rotation of power lines can lead to excess strain and potential for line snapping.[15,16] Veerakumar et al. conducted dynamic, 3-D modeling of ice accretion on power lines as a function of time, testing both rime and glaze icing conditions.[15,30-32] The study utilized a wind tunnel similar to the Lewis IRT, to conduct ice accretion measurements of a power cable. This study highlighted the significance of ice accretion time, as well as the atmospheric conditions present during the icing.[15,29] The temperature strongly influences the type of ice that forms, and time influences the amount. Glaze and rime ice effect powerlines differently. These differences are shown in Figure 1.3, where a cylinder had been covered in both glaze and rime icing. The test found significant differences in the way the layers of each icing type formed.

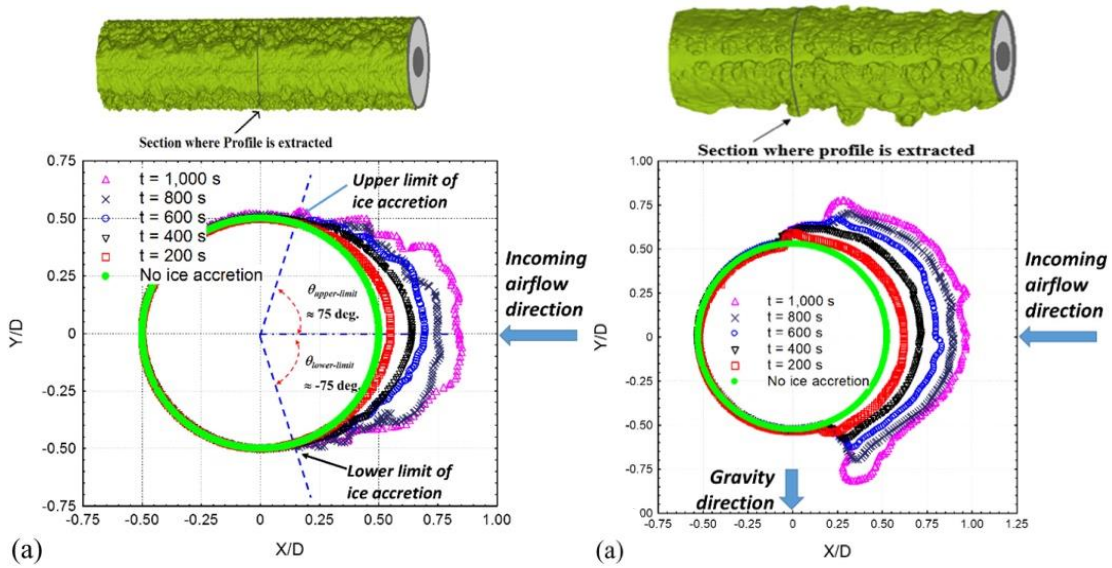

Figure 1.3. Cross-section of rime (*left*) and glaze (*right*) ice accretion on a power cable. Reprinted from reference 15.

The study found that rime ice formation is more localized where droplets impact and instantly freeze.[30-32] The ice accretion formed only on the side of exposure to the incoming droplets, and the ice accretion was more uniform along the entire cable.[15] Oppositely, as seen in Figure 1.3b, the glaze ice is less localized due to the droplets not immediately freezing. This allows the water to flow, and as more layers of ice are accreted, the size and shape of the ice begins to drastically change. The effect of gravity becomes relevant, and the droplets spread, as ice accretion becomes uneven. This was seen in the study when cross-sections were measured at different spots along the cable length. In the rime icing conditions, cross-sections of the ice accretion along the cable were consistent, whereas in the glaze conditions the ice accretion was more random along the entire cable. This delocalization leads to imbalances in the weight of the cable, and can lead to situations where gravity, due to the mass of the ice accreted, will cause strain on the cable, or cause the cable to rotate.[15]

Marine Ice Accretion

Ships and marine infrastructure encounter significant precipitation, but also face unique challenges of their own, such as sea spray.[17-19] Sea spray occurs on a ship or offshore structure when sea water is aerosolized and impacts the stucture.[6,34] When a ship breaks a wave, the sea water is aerosolized into clouds of droplets that impact the ship, and if conditions are right, will cause ice accretion.[36] Offshore structures primarily encounter wind-generated sea spray rather than wave-generated spray.[33] Due to the serious safety threat posed by marine ice accretion, significant research was conducted to model and measure it.[35-38] Temperature, droplet size, wind speed, and ship size are a few variables that govern the wave-generated ice accretion that can occur on a ship.

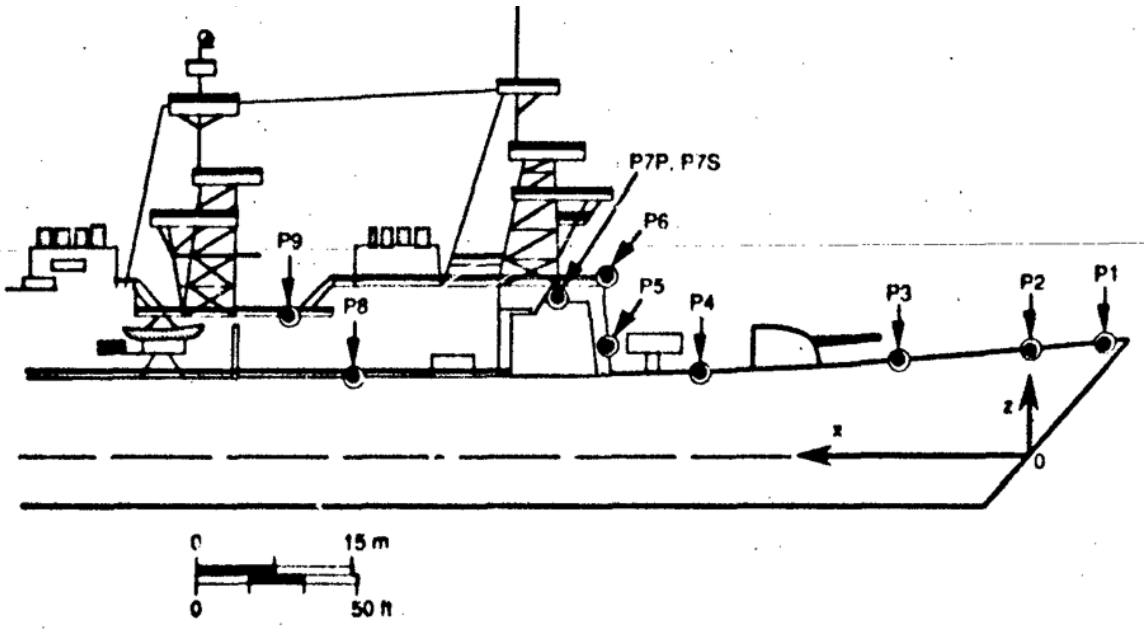

Figure 1.4. Preferrable locations for the icing measurement equipment. Reprinted from reference 40.

Similar to other infrastructure, the ice accretion on ships and offshore structures has been modeled and compared to experimental field data. One study was conducted where ice accretion data was collected on the USCGC *Midgett.*[40] The *Midgett* was a Coast Guard cutter that patrolled

the northern seas near Alaska, an area in which ice accretion is prevalent. Measuring equipment was placed in various locations on the ship to measure the spray flux and ice accretion (Figure 1.4).[40,43] Additionally, video equipment is commonly used to record impact of water on the bow as a ship breaks waves, as well as the water temperature and salinity.[40,43] The combination of video and measuring equipment allows for in depth analysis of the ice accretion that occurs due to wave-generated sea spray.[39,40-43] The spray measurements examine variables such as ship course and speed, wind direction and speed, and droplet diameter.[40] The study found that the bow of the ship, as well as forward sections of the superstructure, had the most exposure to sea spray, and therefore, the most ice accretion. The complexity of the ice accretion process, as well as the variety of infrastructure that it effects, makes mitigation methods difficult. Deicing methods and new materials are being developed to limit ice accretion, involving the physical and chemical modification of surfaces. These modifications include coatings with surface modifying additives or designing materials with micro textures that are not conducive to wetting.

Icing Mitigation Methods - Modification of Surface Chemistry, Topology, and Modulus

Multiple different approaches can be taken when creating icephobic coatings (Figure 1.5). Some methods involve designing materials with low modulus, or hollow regions that promote crack propagation.[54] Other methods rely on surface modification, whether that be by changing the surface chemistry, or topology, to achieve a material with low ice adhesion.[53-55]

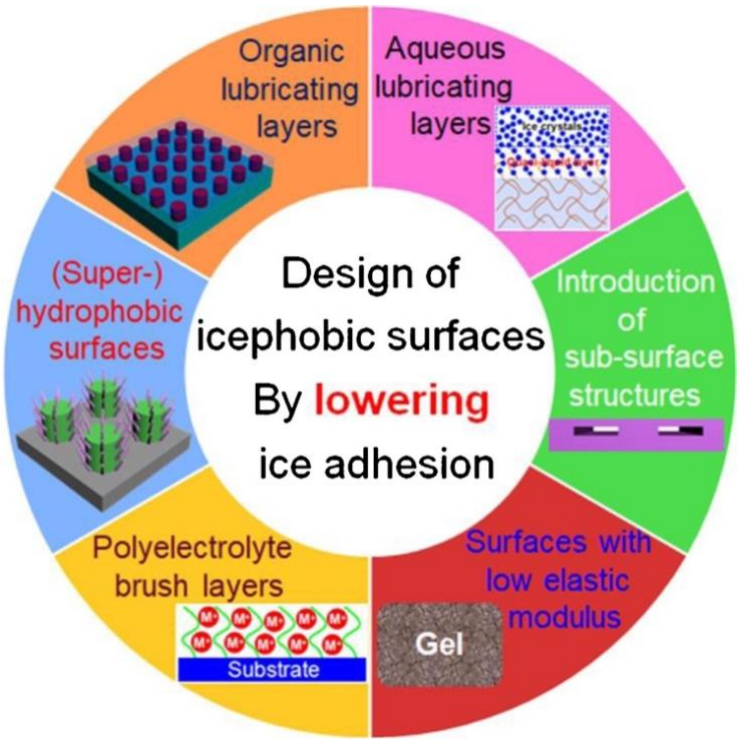

Figure 1.5. Design methods of icephobic materials. Reprinted from reference 54.

Polydimethylsiloxane (PDMS) Icephobic Materials

Changes to surface chemistry are often done with the use of fluorinated or silicone-based materials, such as polydimethylsiloxane (PDMS).[44] These materials can be incorporated through grafting onto the backbone of the system, or added as a lubrication layer.[54,57,58,72] Fluorinated polymers have shown to be successful in creating ice-phobic coatings. [44-46,50] Recently, concerns of negative environmental and health effects from the production and use of fluorinated polymers have arisen.[47,49] Due to this, some focus has moved toward fluorine-free materials.[48,51] Polydimethylsiloxane (PDMS) is an additive widely used to create icephobic or ice releasing coatings.[55,56] It has low surface energy, and is non-toxic, which is beneficial for use in marine applications.[52,53] PDMS is used in icephobic coatings due to its very low surface energy. Low surface energy lowers the ability of ice to adhere to the surface.[65] This can prevent water from wetting a surface long enough for ice to form. The theory is: if the water cannot wet the surface

when water encounters the surface, the water will run off the surface before ice can form. If ice does form, the low surface energy will allow for the easy removal of the ice. In some cases, the weight of the ice itself provides sufficient force.[64,66]

Superhydrophobic Materials

Another method of designing icephobic coatings uses superhydrophobic surfaces.[59] Superhydrophobic surfaces have a water contact angle greater than 150°, and often have a low sliding angle (<10°).[67,68]

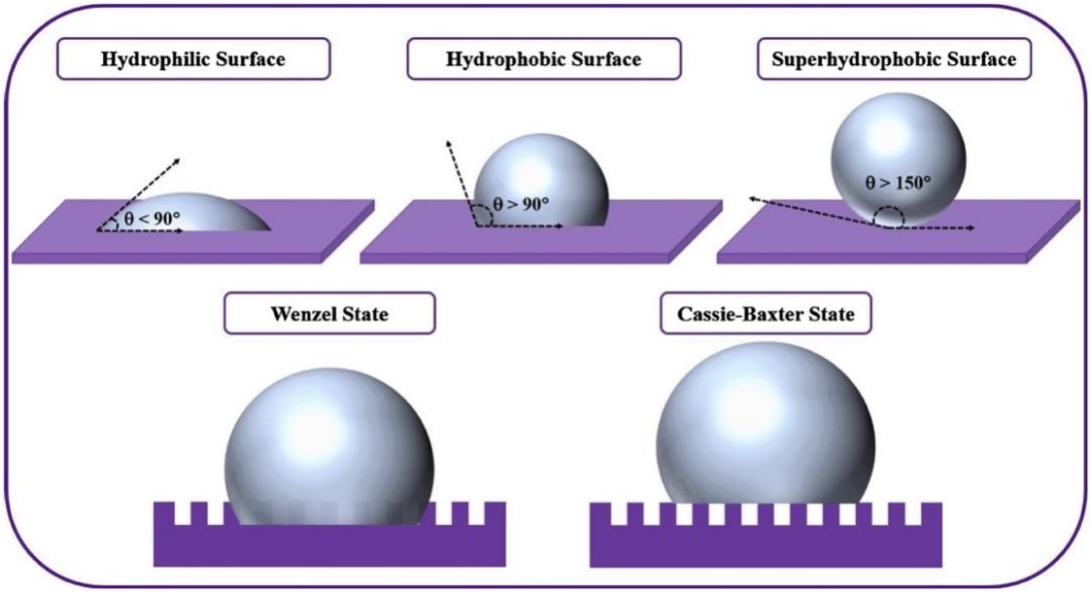

Figure 1.6. Diagram of superhydrophobic surfaces and surfaces classified on contact angle (Θ). Reprinted from reference 63.

Fabrication of micro-textures to create a superhydrophobic surface can prevent the wetting of a surface.[60-62,67,76] Typically, superhydrophobic materials have a highly textured surface at the micro or nano scale. While the topography can affect the ice adhesion of a material, the surface chemistry is still relevant.[76] Micro-texturing increases a material's surface area. This leads to an amplification of the surface properties that are present in the material.[76] There are three classifications for superhydrophobic materials. The classification depends on how a droplet interacts with the surfaces. Ice releasing properties of a superhydrophobic

materials depend on the way droplets interact with the surface. The Cassie-Baxter state (Figure 1.6) is where droplets rest above pockets of air that are trapped between the roughness of the material's surface. Materials that have these types of surfaces have very low sliding angle and can self-clean.[63] Additionally, the ice adhesion of these materials is generally low due to the limited contact of water/ice with the surface. The Wenzel state is where the water has penetrated into the surface roughness. If freezing occurs in this state, the ice adhesion can be much higher due to the increased surface area in contact with the water droplet.[74] This highlights the fact that contact angle results are not always representative of ice adhesion properties. Finally, there is the Marmur state, which is where the droplet is suspended above the air and partially penetrates into the surface roughness.[75] These different states depend on the droplet substance, as well as the shape and size of the microstructures present on the surface.[71]

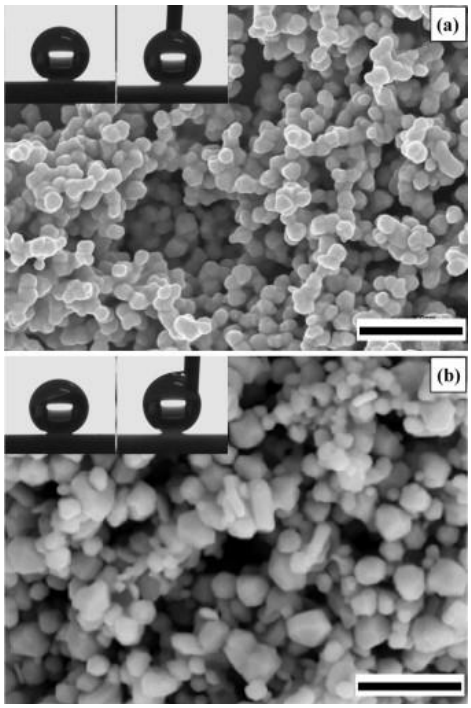

Figure 1.7. SEM and contact angle images of two Ag nanoparticle surface samples (a) 80-400nm particles (b) 100-600nm particles. Scale bar represents 1 μm. Reprinted from reference 73.

Hybrid Icephobic Coatings

Some studies are working to combine both approaches to make hybrid materials possible, which can further improve the anti-icing or ice releasing properties of a material.[55,69] Yu et al. designed a polyacrylate/PDMS graft copolymer to create a hybrid surface. Low surface energy is obtained by the PDMS chains that are integrated into the polyacrylate system. When used in conjunction, the two materials separate into different phases, and create a surface roughness that additionally aids in the lowering of ice adhesion onto the surface.[70,76] Li et al. created a PDMS/modified nano-silica hybrid superhydrophobic coating which had a well-defined microstructure. When exposed to icing environments, the hybrid coating accreted much less ice than the control.[69] Yang et al. created a hybrid surface by modifying ZnO particles with PDMS. The coatings exhibited a very high contact angle. A unique aspect of this study was the exploration of the effects of repeated freezing and thawing on the contact angle. Over multiple cycles, the structure of the surface can become worn down, and the material can begin to lose hydrophobicity.[68] This was not found to be the case for the ZnO/PDMS surface surface.[68]

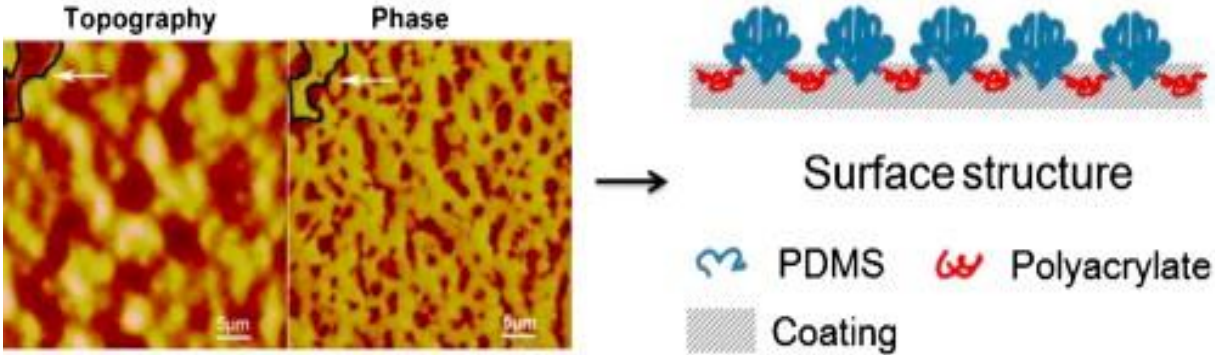

Figure 1.8. Diagram showing topographical and chemical modification of a surface using a grafted PDMS/polyacrylate polymer. Reprinted from reference 70.

Ryu et al. designed a hybrid material through a unique process. This involved creating an elastomeric PDMS material that was molded over a lotus leaf to create a micro-textured surface.[77] This procedure combined three approaches to designing icephobic materials: a PDMS

lubricating layer, low elastic modulus, and a microtextured surface.[54,77] Psarski et al. created a brush-like icephobic material by grating fluoroalkylsilane chains of different lengths onto epoxy coatings using vapor deposition. The study found that the length of fluoroalkylsilane greatly influenced the surface roughness, contact angle, and ice releasing properties.[78]

Low Interfacial Toughness Materials

While having a low ice adhesion force is necessary for developing icephobic coatings, further testing is needed to determine if a material has potential for use in real world scenarios. The infrastructure often affected by icing (aircraft, wind turbines and ships) accumulates large pieces of ice, and removal can be difficult, expensive, and time consuming. Interfacial toughness is the ability of an interface to resist crack propagation, and is dependent on factors such as surface roughness, surface chemistry, and temperature.[66,79] While this study conducted by Reedy et al. explored the interface between a substrate and an epoxy coating, the concepts can be applied to the interface between ice and a material or coating. When studying icing on larger structures, the size of the ice is important for understanding the adhesive forces and removal. The removal of smaller pieces of ice is dependent on the adhesion strength of the ice on the material. For larger pieces of ice, the removal is dependent on the interfacial toughness.[66,80] This change between which factor controls adhesion is referred to as the critical length. Critical length will be different depending on the surface.[66,80] Critical length (L_c) can be determined by measuring the force required to remove ice of increasing length that has constant width and height (h).[66] Beyond a certain length (L_c), the force (critical force) to remove the ice will plateau. With the critical length and critical force known, the interfacial toughness can be determined.

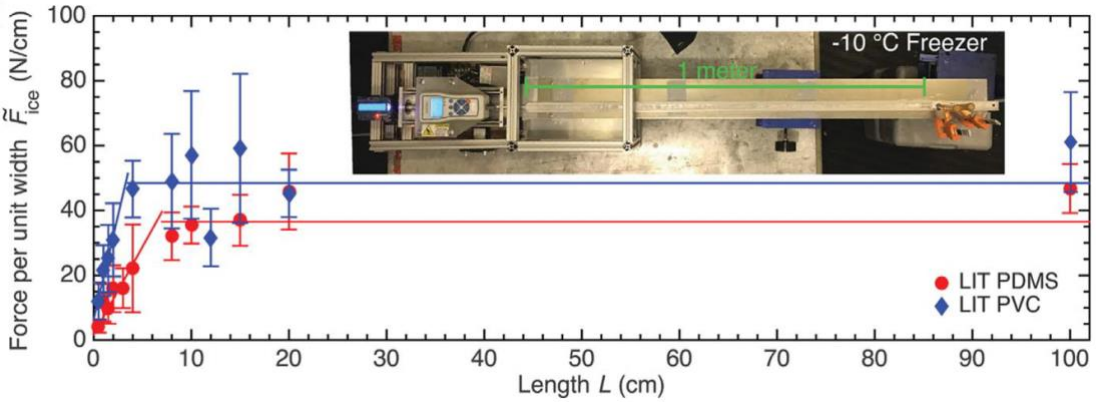

Figure 1.9. Graph of critical force vs critical length. Reprinted from reference 66.

The graph in Figure 1.9 shows the plateauing of the force that occurs after the critical length is reached. After this critical length, interfacial strength controls the adhesion of the ice onto the surface.[66,80,81] Understanding whether shear strength or interfacial strength will govern the release of ice accreted on a material, helps to design the proper materials for the desired application. Mohseni et al. measured the interfacial toughness and surface roughness of two quasicrystal coatings. One of the goals was to determine the effect that surface roughness has on the interfacial toughness of a material. The study found that while increased roughness can lead to lower shear strength, the increase in surface roughness leads to higher interfacial toughness.[81] When developing materials and coatings to solve these issues, it is important to understand the areas of application as well as the specific end goal of the material. Golovin et al. prepared low interfacial toughness samples (LIT) from thin coatings (~1 μm) of polydimethylsiloxane, polyvinylchloride, and polystyrene. The coatings were able to shed a piece of ice 1m x 1m, with the weight of the ice alone.[66] Coatings with similarly low interfacial toughness could provide an excellent solution to large-scale, passive deicing.

Biofouling and Ice Releasing Coatings

In addition to ice accretion, biofouling is another serious issue that ships face. This occurs when biological organisms adhere and build up on a surface that is in water.[82] These organisms vary in size and consist of bacteria, algae, and other common marine life. Antifouling and fouling release coatings have long been used to mitigate the accumulation of biological organisms on ships. Original technologies utilized biocides but were eventually banned due to ecological concerns. Modern antifouling coatings are more focused on lowering adhesion to the surface rather than prevention of attachment.[82] Ship hulls that suffer from ice accretion are also at risk for biofouling, so the ability to use one coating to solve both issues is desirable. Studies have been conducted exploring the antifouling properties of ice releasing coatings and vice versa.[83] Some strategies, such as designing low surface energy coatings, have shown promising results for the prevention of fouling and ice accretion. The main challenge comes from the large number of known biofouling organisms that accumulate on ships and other infrastructure at sea. Upadhyay et al. explored the ice releasing properties of amphiphilic antifouling coatings to see if a correlation could be made between the properties. The study found that some of the amphiphilic coatings showed lowered biofouling and ice accretion. The study concluded that the ratio of hydrophobic and hydrophilic moieties heavily influenced the fouling and ice releasing properties of the coatings.[83]

Research Scope

The goal of this research was to develop an ice releasing coating for ship hulls, through the modification of an epoxy-siloxane using polysiloxane oil additives. Additionally, the anti-fouling/fouling release properties of the materials were studied with the intent of exploring the correlations between anti-icing and anti-fouling coatings. Epoxy-siloxanes benefit from the

properties that each part provides to the combined system. Where the epoxy lacks in UV resistance, the siloxane excels. Oppositely, where the siloxane lacks in durability and chemical resistance, the epoxy excels. Previously, the coating used for the upper hull and superstructure of ships was an epoxy base coat with a polyurethane topcoat. The drawback of this system is the requirement for two coatings to be applied, which takes longer and leads to higher costs. The epoxy-siloxane system solves both drawbacks. As ships are migrating further north, the coatings applied to ships need to have improved anti-icing/ice releasing properties. Utilizing durable coatings with low interfacial toughness could prevent large scale ice accretion on ships exposed to icing conditions. The epoxy-siloxane coating with additional PDMS is a simple method to achieve materials with such properties, while maintaining the mechanical/weathering durability needed for ships.

References

(1) Macklin, W.; Payne, G. A theoretical study of the ice accretion process. *Quarterly Journal of the Royal Meteorological Society* **1967**, *93* (396), 195-213.

(2) Handbook, A. I. Civil Aviation Authority. *Lower Hutt, New Zealand* **2000**.

(3) Louchez, P.; Laforte, J.-L.; Bouchard, G.; Farzaneh, M. Laboratory evaluation of aircraft ground de/antiicing products. In *The Fourth International Offshore and Polar Engineering Conference*, 1994; OnePetro.

(4) Makkonen, L.; Laakso, T.; Marjaniemi, M.; Finstad, K. J. Modelling and prevention of ice accretion on wind turbines. *Wind engineering* **2001**, *25* (1), 3-21.

(5) Bragg, M.; Hutchison, T.; Merret, J. Effect of ice accretion on aircraft flight dynamics. In *38th Aerospace Sciences Meeting and Exhibit*, 2000; p 360.

(6) Lundqvist, J.-E.; Udin, I. *Ice accretion on ships with special emphasis on Baltic conditions*; SMHI, 1977.

(7) Pauschenwein, G. J.; Reichl, C.; Windholz, B.; Moretti, I.; Monsberger, M. CFD simulations for solar collectors including condensation and ice accretion. 2010; Eurosun.

(8) Lv, J.; Song, Y.; Jiang, L.; Wang, J. Bio-inspired strategies for anti-icing. *ACS nano* **2014**, *8* (4), 3152-3169.

(9) Cornell, J. S.; Pillard, D. A.; Hernandez, M. T. Comparative measures of the toxicity of component chemicals in aircraft deicing fluid. *Environmental Toxicology and Chemistry: An International Journal* **2000**, *19* (6), 1465-1472.

(10) Gruden, C. L.; Dow, S. M.; Hernandez, M. T. Fate and toxicity of aircraft deicing fluid additives through anaerobic digestion. *Water Environment Research* **2001**, *73* (1), 72-79.

(11) Corsi, S. R.; Geis, S. W.; Loyo-Rosales, J. E.; Rice, C. P.; Sheesley, R. J.; Failey, G. G.; Cancilla, D. A. Characterization of aircraft deicer and anti-icer components and toxicity in airport snowbanks and snowmelt runoff. *Environmental science & technology* **2006**, *40* (10), 3195-3202.

(12) Castro, S.; Davis, L. C.; Erickson, L. E. Natural, cost-effective, and sustainable alternatives for treatment of aircraft deicing fluid waste. *Environmental progress* **2005**, *24* (1), 26-33.

(13) Corsi, S. R.; Geis, S. W.; Loyo-Rosales, J. E.; Rice, C. P. Aquatic toxicity of nine aircraft deicer and anti-icer formulations and relative toxicity of additive package ingredients alkylphenol ethoxylates and 4, 5-methyl-1H-benzotriazoles. *Environmental science & technology* **2006**, *40* (23), 7409-7415.

(14) Makkonen, L. Modeling of ice accretion on wires. *Journal of Applied Meteorology and Climatology* **1984**, *23* (6), 929-939.

(15) Veerakumar, R.; Gao, L.; Liu, Y.; Hu, H. Dynamic ice accretion process and its effects on the aerodynamic drag characteristics of a power transmission cable model. *Cold Regions Science and Technology* **2020**, *169*, 102908.

(16) Fu, P.; Farzaneh, M.; Bouchard, G. Two-dimensional modelling of the ice accretion process on transmission line wires and conductors. *Cold Regions Science and Technology* **2006**, *46* (2), 132-146.

(17) Mintu, S.; Molyneux, D. Ice accretion for ships and offshore structures. Part 2–Compilation of data. *Ocean Engineering* **2022**, *248*, 110638.

(18) Bodaghkhani, A.; Dehghani, S.-R.; Muzychka, Y. S.; Colbourne, B. Understanding spray cloud formation by wave impact on marine objects. *Cold Regions Science and Technology* **2016**, *129*, 114-136.

(19) Ryerson, C. C. Superstructure spray and ice accretion on a large US Coast Guard cutter. *Atmospheric research* **1995**, *36* (3-4), 321-337.

(20) Qin, C. C.; Mulroney, A. T.; Gupta, M. C. Anti-icing epoxy resin surface modified by spray coating of PTFE Teflon particles for wind turbine blades. *Materials Today Communications* **2020**, *22*, 100770.

(21) Mingione, G.; Brandi, V. Ice accretion prediction on multielement airfoils. *Journal of Aircraft* **1998**, *35* (2), 240-246.

(22) Bragg, M. Aircraft aerodynamic effects due to large droplet ice accretions. In *34th Aerospace Sciences Meeting and Exhibit*, 1996; p 932.

(23) Pokhariyal, D.; Bragg, M.; Hutchison, T.; Merret, J. Aircraft flight dynamics with simulated ice accretion. In *39th Aerospace Sciences Meeting and Exhibit*, 2001; p 541.

(24) Lynch, F. T.; Khodadoust, A. Effects of ice accretions on aircraft aerodynamics. *Progress in Aerospace Sciences* **2001**, *37* (8), 669-767.

(25) Shin, J.; BOND, T. Results of an icing test on a NACA 0012 airfoil in the NASA Lewis icing research tunnel. In *30th Aerospace Sciences Meeting and Exhibit*, 1992; p 647.

(26) Tran, P.; Brahimi, M.; Tezok, F.; Paraschivolu, I. Numerical simulation of ice accretion on multiple element configurations. In *34th Aerospace Sciences Meeting and Exhibit*, 1996; p 869.

(27) Homola, M. C.; Nicklasson, P. J.; Sundsbø, P. A. Ice sensors for wind turbines. *Cold regions science and technology* **2006**, *46* (2), 125-131.

(28) Li, Y.; Wang, S.; Liu, Q.; Feng, F.; Tagawa, K. Characteristics of ice accretions on blade of the straight-bladed vertical axis wind turbine rotating at low tip speed ratio. *Cold Regions Science and Technology* **2018**, *145*, 1-13.

(29) Zdero, R.; Turan, O. F. The effect of surface strands, angle of attack, and ice accretion on the flow field around electrical power cables. *Journal of wind engineering and industrial aerodynamics* **2010**, *98* (10-11), 672-678.

(30) Anderson, D. Rime-, mixed-and glaze-ice evaluations of three scaling laws. In *32nd Aerospace Sciences Meeting and Exhibit*, 1994; p 718.

(31) Makkonen, L. Models for the growth of rime, glaze, icicles and wet snow on structures. *Philosophical Transactions of the Royal Society of London. Series A: Mathematical, Physical and Engineering Sciences* **2000**, *358* (1776), 2913-2939.

(32) Zhang, X.; Min, J.; Wu, X. Model for aircraft icing with consideration of property-variable rime ice. *International Journal of Heat and Mass Transfer* **2016**, *97*, 185-190.

(33) Young, I.; Zieger, S.; Babanin, A. V. Global trends in wind speed and wave height. *Science* **2011**, *332* (6028), 451-455.

(34) Sultana, K.; Dehghani, S.; Pope, K.; Muzychka, Y. A review of numerical modelling techniques for marine icing applications. *Cold Regions Science and Technology* **2018**, *145*, 40-51.

(35) Lozowski, E.; Zakrzewski, W. An Integrated Ship Spraying/Icing Model. In *Milestone Report No. 2. Contract Report by the University of Alberta, Edmonton, to USA Cold Regions Research and Engineering Laboratory*, 1990.

(36) Iwata, S. Ice accumulation on ships. *Selected Papers, J of Soc of Naval Arch of Japan* **1973**, *11*.

(37) Dehghani-Sanij, A.; Dehghani, S.; Naterer, G.; Muzychka, Y. Marine icing phenomena on vessels and offshore structures: Prediction and analysis. *Ocean engineering* **2017**, *143*, 1-23.

(38) Dehghani-Sanij, A.; Dehghani, S.; Naterer, G.; Muzychka, Y. Sea spray icing phenomena on marine vessels and offshore structures: Review and formulation. *Ocean engineering* **2017**, *132*, 25-39.

(39) Kultashev, Y.; Malakhov, N.; Panov, V.; Shmidt, M. Spray icing of MFT and MFTF fishing vessels. *US Army CRREL Draft Translation* **1974**, *411*, 127-139.

(40) Ryerson, C. C.; Longo, P. D. *Ship Superstructure Icing: Data Collection and Instrument Performance on USCGC MIDGETT Research Cruise*; COLD REGIONS RESEARCH AND ENGINEERING LAB HANOVER NH, 1992.

(41) Ryerson, C. C.; Gow, A. J. Crystalline structure and physical properties of ship superstructure spray ice. *Philosophical Transactions of the Royal Society of London. Series A: Mathematical, Physical and Engineering Sciences* **2000**, *358* (1776), 2847-2871.

(42) Andreas, E. L. A new sea spray generation function for wind speeds up to 32 ms− 1. *Journal of Physical Oceanography* **1998**, *28* (11), 2175-2184.

(43) Itagaki, K. Icing on Ships and Stationary Structures under Maritime Conditions. *USA Cold Regions Research and Engineering Laboratory, CRREL Spec. Rep* **1977**, 77-27.

(44) Li, H.; Li, X.; Luo, C.; Zhao, Y.; Yuan, X. Icephobicity of polydimethylsiloxane-b-poly (fluorinated acrylate). *Thin Solid Films* **2014**, *573*, 67-73.

(45) Zhang, K.; Li, X.; Zhao, Y.; Zhu, K.; Li, Y.; Tao, C.; Yuan, X. UV-curable POSS-fluorinated methacrylate diblock copolymers for icephobic coatings. *Progress in Organic Coatings* **2016**, *93*, 87-96.

(46) Tao, C.; Li, X.; Liu, B.; Zhang, K.; Zhao, Y.; Zhu, K.; Yuan, X. Highly icephobic properties on slippery surfaces formed from polysiloxane and fluorinated POSS. *Progress in Organic Coatings* **2017**, *103*, 48-59.

(47) Lohmann, R.; Cousins, I. T.; DeWitt, J. C.; Gluge, J.; Goldenman, G.; Herzke, D.; Lindstrom, A. B.; Miller, M. F.; Ng, C. A.; Patton, S. Are fluoropolymers really of low concern for human and environmental health and separate from other PFAS? *Environmental Science & Technology* **2020**, *54* (20), 12820-12828.

(48) Wu, X.; Zhao, X.; Ho, J. W. C.; Chen, Z. Design and durability study of environmental-friendly room-temperature processable icephobic coatings. *Chemical Engineering Journal* **2019**, *355*, 901-909.

(49) Cadore, A.; Chou, C.-H.; Jones, D. G.; Llados, F.; Pohl, H. R. Draft toxicological profile for perfluoroalkyls. **2009**.

(50) Yang, S.; Xia, Q.; Zhu, L.; Xue, J.; Wang, Q.; Chen, Q.-m. Research on the icephobic properties of fluoropolymer-based materials. *Applied Surface Science* **2011**, *257* (11), 4956-4962.

(51) Kasapgil, E.; Anac, I.; Erbil, H. Y. Transparent, fluorine-free, heat-resistant, water repellent coating by infusing slippery silicone oil on polysiloxane nanofilament layers prepared by gas phase reaction of n-propyltrichlorosilane and methyltrichlorosilane. *Colloids and Surfaces A: Physicochemical and Engineering Aspects* **2019**, *560*, 223-232.

(52) Hobbs, E.; Keplinger, M.; Calandra, J. Toxicity of polydimethylsiloxanes in certain environmental systems. *Environmental research* **1975**, *10* (3), 397-406.

(53) Nendza, M. Hazard assessment of silicone oils (polydimethylsiloxanes, PDMS) used in antifouling-/foul-release-products in the marine environment. *Marine Pollution Bulletin* **2007**, *54* (8), 1190-1196.

(54) He, Z.; Zhuo, Y.; Wang, F.; He, J.; Zhang, Z. Design and preparation of icephobic PDMS-based coatings by introducing an aqueous lubricating layer and macro-crack initiators at the ice-substrate interface. *Progress in Organic Coatings* **2020**, *147*, 105737.

(55) Bleszynski, M.; Woll, R.; Middleton, J.; Kumosa, M. Effects of crosslinking, embedded TiO2 particles and extreme aging on PDMS icephobic barriers. *Polymer degradation and stability* **2019**, *166*, 272-282.

(56) He, Z.; Zhuo, Y.; He, J.; Zhang, Z. Design and preparation of sandwich-like polydimethylsiloxane (PDMS) sponges with super-low ice adhesion. *Soft Matter* **2018**, *14* (23), 4846-4851.

(57) Shamshiri, M.; Jafari, R.; Momen, G. Icephobic properties of aqueous self-lubricating coatings containing PEG-PDMS copolymers. *Progress in Organic Coatings* **2021**, *161*, 106466.

(58) Gao, S.; Liu, B.; Peng, J.; Zhu, K.; Zhao, Y.; Li, X.; Yuan, X. Icephobic durability of branched PDMS slippage coatings co-cross-linked by functionalized POSS. *ACS applied materials & interfaces* **2019**, *11* (4), 4654-4666.

(59) Pan, S.; Wang, N.; Xiong, D.; Deng, Y.; Shi, Y. Fabrication of superhydrophobic coating via spraying method and its applications in anti-icing and anti-corrosion. *Applied Surface Science* **2016**, *389*, 547-553.

(60) Zhou, B.; Tian, J.; Wang, C.; Gao, Y.; Wen, W. A facile and cost-effective approach to engineer surface roughness for preparation of large-scale superhydrophobic substrate with high adhesive force. *Applied Surface Science* **2016**, *389*, 679-687.

(61) Brassard, J.-D.; Sarkar, D. K.; Perron, J.; Audibert-Hayet, A.; Melot, D. Nano-micro structured superhydrophobic zinc coating on steel for prevention of corrosion and ice adhesion. *Journal of colloid and interface science* **2015**, *447*, 240-247.

(62) Dunn, A.; Wasley, T. J.; Li, J.; Kay, R. W.; Stringer, J.; Smith, P. J.; Esenturk, E.; Connaughton, C.; Shephard, J. D. Laser textured superhydrophobic surfaces and their applications for homogeneous spot deposition. *Applied Surface Science* **2016**, *365*, 153-159.

(63) Latthe, S. S.; Sutar, R. S.; Bhosale, A. K.; Nagappan, S.; Ha, C.-S.; Sadasivuni, K. K.; Liu, S.; Xing, R. Recent developments in air-trapped superhydrophobic and liquid-infused slippery surfaces for anti-icing application. *Progress in Organic Coatings* **2019**, *137*, 105373.

(64) Dotan, A.; Dodiuk, H.; Laforte, C.; Kenig, S. The relationship between water wetting and ice adhesion. *Journal of Adhesion Science and Technology* **2009**, *23* (15), 1907-1915.

(65) Lamberti, A.; Quaglio, M.; Sacco, A.; Cocuzza, M.; Pirri, C. Surface energy tailoring of glass by contact printed PDMS. *Applied surface science* **2012**, *258* (23), 9427-9431.

(66) Golovin, K.; Dhyani, A.; Thouless, M.; Tuteja, A. Low–interfacial toughness materials for effective large-scale deicing. *Science* **2019**, *364* (6438), 371-375.

(67) Barthlott, W.; Neinhuis, C. Purity of the sacred lotus, or escape from contamination in biological surfaces. *Planta* **1997**, *202* (1), 1-8.

(68) Yang, C.; Wang, F.; Li, W.; Ou, J.; Li, C.; Amirfazli, A. Anti-icing properties of superhydrophobic ZnO/PDMS composite coating. *Applied Physics A* **2016**, *122* (1), 1-10.

(69) Li, J.; Zhao, Y.; Hu, J.; Shu, L.; Shi, X. Anti-icing performance of a superhydrophobic PDMS/modified nano-silica hybrid coating for insulators. *Journal of adhesion science and technology* **2012**, *26* (4-5), 665-679.

(70) Yu, D.; Zhao, Y.; Li, H.; Qi, H.; Li, B.; Yuan, X. Preparation and evaluation of hydrophobic surfaces of polyacrylate-polydimethylsiloxane copolymers for anti-icing. *Progress in Organic Coatings* **2013**, *76* (10), 1435-1444.

(71) Cansoy, C. E.; Erbil, H. Y.; Akar, O.; Akin, T. Effect of pattern size and geometry on the use of Cassie–Baxter equation for superhydrophobic surfaces. *Colloids and Surfaces A: Physicochemical and Engineering Aspects* **2011**, *386* (1-3), 116-124.

(72) Zhu, L.; Xue, J.; Wang, Y.; Chen, Q.; Ding, J.; Wang, Q. Ice-phobic coatings based on silicon-oil-infused polydimethylsiloxane. *ACS applied materials & interfaces* **2013**, *5* (10), 4053-4062.

(73) Kulinich, S.; Farzaneh, M. Ice adhesion on super-hydrophobic surfaces. *Applied Surface Science* **2009**, *255* (18), 8153-8157.

(74) Huré, M.; Olivier, P.; Garcia, J. Effect of Cassie-Baxter versus Wenzel states on ice adhesion: A fracture toughness approach. *Cold Regions Science and Technology* **2022**, *194*, 103440.

(75) Si, Y.; Guo, Z. Superhydrophobic nanocoatings: from materials to fabrications and to applications. *Nanoscale* **2015**, *7* (14), 5922-5946.

(76) Zou, M.; Beckford, S.; Wei, R.; Ellis, C.; Hatton, G.; Miller, M. Effects of surface roughness and energy on ice adhesion strength. *Applied surface science* **2011**, *257* (8), 3786-3792.

(77) Ryu, B.-H.; Kim, D.-E. Development of highly durable and low friction micro-structured PDMS coating based on bio-inspired surface design. *CIRP Annals* **2015**, *64* (1), 519-522.

(78) Psarski, M.; Pawlak, D.; Grobelny, J.; Celichowski, G. Relationships between surface chemistry, nanotopography, wettability and ice adhesion in epoxy and SU-8 modified with fluoroalkylsilanes from the vapor phase. *Applied Surface Science* **2019**, *479*, 489-498.

(79) Reedy, E. D.; Stavig, M. E. Interfacial toughness: dependence on surface roughness and test temperature. *International Journal of Fracture* **2020**, *222* (1), 1-12.

(80) Zarasvand, K. A.; Mohseni, M.; Golovin, K. Cohesive zone analysis of cylindrical ice adhesion: Determining whether interfacial toughness or strength controls fracture. *Cold Regions Science and Technology* **2021**, *183*, 103219.

(81) Mohseni, M.; Recla, L.; Mora, J.; Gallego, P. G.; Aguero, A.; Golovin, K. Quasicrystalline Coatings Exhibit Durable Low Interfacial Toughness with Ice. *ACS Applied Materials & Interfaces* **2021**, *13* (30), 36517-36526.

(82) Yebra, D. M.; Kiil, S.; Dam-Johansen, K. Antifouling technology—past, present and future steps towards efficient and environmentally friendly antifouling coatings. *Progress in organic coatings* **2004**, *50* (2), 75-104.

(83) Upadhyay, V.; Galhenage, T.; Battocchi, D.; Webster, D. Amphiphilic icephobic coatings. *Progress in Organic Coatings* **2017**, *112*, 191-199.

CHAPTER 2. POLYSILOXANE OIL MODIFIED EPOXY-SILOXANE COATINGS

Introduction

Epoxy coatings remain a critical technology used in many industries. They are used for the protection and decoration of various materials such as metals, wood, and concrete.[1] The main utility of epoxy coatings comes from their durability, chemical resistance, and corrosion prevention.[1] In addition to coating applications, epoxies are a popular flooring material, where they provide long lasting protection from impact, abrasion, and harsh substances[1]. The most commonly used epoxy resin bisphenol-A, and other aromatic epoxies, are vulnerable to weather, specifically when exposed to ultraviolet (UV) radiation.[2] The aromatic rings absorb UV radiation which leads to degradation of the coating.[1,3] To protect the decorative finish of epoxy coatings that are exposed to UV, a top coating can be added to shield the epoxy from direct exposure. This top coating is commonly a durable polyurethane. However, the synthesis of polyurethanes requires the handling of toxic isocyanates, so efforts have been made to avoid using these coatings.[4,5] Beyond this, the problem with the two-part solution is that it involves applying multiple coats, increasing material and application costs. Thus, an ongoing goal is to find a way to combine these properties into a single coating system.

Epoxy-siloxane coatings are a relatively new technology that incorporate the durability of epoxy resins with the weather resistance of silicones. This is a desirable coating system that avoids the additional cost of using a topcoat to provide the desired level of protection. Epoxy-siloxane coatings are generally comprised of a non-aromatic epoxy resin, an organosilane, a polysiloxane, and an aminoalkylsilane.[1] The amine groups of the aminoalkylsilane react with the epoxy through an epoxy-amine reaction, and the silane groups react with the organosilane and polysiloxane through hydrolytic polycondensation, creating a crosslinked epoxy-siloxane

coating. The benefit of this system is a highly durable coating, that is weather resistant due to the selection of an aliphatic/cycloaliphatic epoxy resin and the siloxanes present.

A significant challenge for the military, transportation, and energy industries is snow/ice accumulation.[6] Ice accretion on an aircraft can have catastrophic effects. Ice can interfere with flight control mechanics or worse, hinder the generation of lift. On wind turbines, ice accretion can create imbalances between the turbine blades, leading to inefficiency or potential failure. Ice accretion on power lines can causing straining on the line and eventual snapping. Ice accretion on a ship's superstructure can fall, posing a serious risk of injury or death to crew members. As naval ships and transportation vessels move further north into arctic shipping lanes, ice mitigation strategies will become more important for efficiency and safety.

Ships also face the issue of fouling. Biofouling is the buildup of marine organisms on a surface that is in the water.[13] There are over known 4,000 marine organisms capable of fouling. This makes mitigation methods quite difficult.[12,13] Biofouling consists of micro-organisms such as bacteria and algae up to macro-organisms like barnacles and mussels. Uncontrolled biofouling can lead to increased drag, accelerated corrosion, and the transfer of invasive species to other ecosystems.[12-14] Previously, coatings containing biocides, such as tributyltin oxide, were used to prevent the accumulation of biofouling. These coatings were successful in preventing the attachment of marine organisms, but it was later discovered that they were harming the surrounding ecosystem. In 1980, the International Maritime Organization banned the use of these coatings.[12,13] This led to the development of non-toxic fouling release coatings. Silicone oil additives in a silicone elastomer became popular as a non-toxic ship hull coating.[12] The presence of silicone oil creates a lubricating layer that prevents strong attachment of marine organisms and

allows for easy removal.[15,16] Incorporation of amphiphilic silicone oil creates a heterogenous surface that makes the attachment of marine organisms more difficult.

Silicone oil additives are also used for creating icephobic coatings.[17,18] Like the fouling release coatings, the silicone oil at the surface lowers the adhesion of ice. Similarities have been identified between ice releasing properties and fouling releasing properties.[19] There has been little overlap between these two coating technologies. Upadhyay et al. conducted an ice adhesion study on a series of amphiphilic coatings that had been characterized using biofouling assays. Some of the coatings that performed well against biofouling also exhibited icephobic characteristics.[19] When using amphiphilic additives, the balance between each moiety is crucial in determining the ice/fouling releasing properties of the material.[19] The findings are promising but need to be researched further to better understand how each moiety is affecting the ice and fouling that attach to the surface.

The goal of this study was to determine if incorporating polysiloxane oil additives into an epoxy-siloxane coatings system could improve the ice-releasing performance of an epoxy-siloxane coating system. A base epoxy-siloxane coating was prepared based on a published patent[1], then, a series of polysiloxane oils were added to determine their effect on the hydrophobicity and ice-adhesion properties of the coatings. The coatings were also evaluated using laboratory assays to determine their fouling-release properties with the intention of drawing correlations between ice releasing and fouling releasing coatings.

Experimental

Materials

Eponex 1510 was purchased from Hexion (OH, USA). DC-3074 was purchased from Dow Chemical Company (MI, USA). The (3-aminopropyl) trimethoxysilane, 97% was

purchased from Sigma Aldrich (MO, USA). The t-butyl acetate was purchased from Alfa Aesar (MA, USA). Methytrimethoxysilane, 99% and PDMS copolymer and homopolymer oils, 4-6% diphenylsiloxane-dimethylsiloxane (3,500-4,000 g mol^{-1}), 18-22% diphenylsiloxane-dimethylsiloxane (1,600-2,400 g mol^{-1}), 8-12% phenylmethylsiloxane-dimethylsiloxane (1,500-1,600 g mol^{-1}), 48-52% phenylmethylsiloxane-dimethylsiloxane (2,200 g mol^{-1}), 45-55% phenylmethylsiloxane-diphenylsiloxane (600-800 g mol^{-1}), phenylmethylsiloxane (2,500-2,700 g mol^{-1}) were purchased from Gelest Inc (PA, USA). All materials were used as provided without any further purification. Intergard 264, Intersleek® 700, Intersleek® 900, and Intersleek® 1100SR were purchased from AkzoNobel, International Paint LLC (TN, USA). Silastic® T2 silicone elastomer was purchased from Dow Corning (MI, USA). Steel and aluminum substrates used were QD-48, QD-36, and A-48 purchased from Q-Lab (OH, USA). The aluminum panels (A-48) were sandblasted and then primed, using spray application, with Intergard 264 marine epoxy primer. Falcon sterile, bacterial grade 24-multiwell plates were purchased from VWR International (PA, USA).

Preparation of Resin Component

The R1 resin was made from a hydrogenated bisphenol-a epoxy resin a methyltrimethoxysilane, and a polysiloxane. The amounts of each are listed below in Table 2.1. These components were mixed using a magnetic stir bar for 1 hour. The epoxide equivalent weight (EEW) of the prepared R1 resin was determined based on ASTM D 1652. EEW titrations were done to determine the EEW of the R1 resin to control stochiometric EEW:AHEW ratios for formulation of the coatings. The AHEW was obtained from the supplier. First, a crystal violet indicator and a 0.1M HBr in glacial acetic acid were prepared. The HBr solution was then

standardized by titration of dried potassium acid phthalate (204.2 g/mol) and four drops of crystal violet indicator. The normality (N) was then determined using the following equation:

$$N = \frac{1000 \times W}{204.2 \times V}$$

W = weight of potassium acid phthalate (g)

V = volume of HBr solution (mL)

Next, 1-2g of R1 resin and four drops of indicator were dissolved in chloroform then the normalized HBr solution was used to titrate the R1 resin and a blank that contained the same amount of chloroform and indicator. Three titrations were conducted and then calculations were done to determine the EEW of the resin using the following equation:

$$EEW = \frac{1000 \times W}{N \times (V - B)}$$

W = sample mass (g)

N = normality of HBr solution

V = volume of HBr for titration (mL)

B = volume of HBr for blank (mL)

Coating Formulations

The base coating was prepared based on a formulation in a published patent.[1] The R1 resin was mixed with the (3-aminopropyl) trimethoxysilane at a 1:1 EEW: AHEW along with adding t-butyl acetate to improve flow Table 2.2. Modification of the base coating was done by adding various non-reactive siloxane copolymer and homopolymer oils to improve the surface properties. These siloxane oils were added in different amounts based on percent weight of the R1 resin.

Table 2.1. R1 resin components

R1 resin	Parts
Eponex 1510	45.72
Gelest Methyltrimethoxysilane	2.97
Dowsil DC-3074	51.31

Table 2.2. Coating formulation amounts and ratios

Component	Amounts (g)	
R1 Resin	10.0	
(3-aminopropyl) trimethoxysilane	2.008	
t-butyl acetate	0.726	
Siloxane Oil	**5%**	**10%**
Various oils used	0.5	1.0

Next, a variety of siloxane copolymer oils at different amounts were incorporated into the coating to observe the differences that the amount of phenyl or methyl content would have on the surface properties of each formulation. The formulation ID and description of each oil composition are in Table 2.3. The formulations with "s" have 50% more solvent (~1.0 g) than the regular formulations. Besides the "s" formulations, the only difference between the formulations is the type and amount of silicone oil added.

Table 2.3. Coating formulations and oil composition

Formulation	Siloxane Oil Composition
Base	No oil additive
5% DPDM-005	(4-6% Diphenylsiloxane)-(Dimethylsiloxane)
10% DPDM-005	
5% DPDM-020	(18-22% Diphenylsiloxane)-(Dimethylsiloxane)
10% DPDM-020	
5% PMDM-010	(8-12% Phenylmethylsiloxane)-(Dimethylsiloxane)
5% PMDM-010s	
10% PMDM-010	
10% PMDM-010s	
5% PMDM-050	(48-52% Phenylmethylsiloxane)-(Dimethylsiloxane)
10% PMDM-050	
5% PMDP-050	(45-55% Phenylmethylsiloxane)-(Diphenylsiloxane)
10% PMDP-050	
10% PM-100	100% Phenylmethysiloxane
5% DM-100	100% Dimethylsiloxane
10% DM-100	

For each formulation, the resin, solvent, hardener, and oil additive were mixed using a magnetic stir plate for 30 minutes before leaving open for 10 minutes to allow off-gassing of the solvent and any bubbles created by the mixing. The panels were cleaned prior to application using hexane and then isopropanol. Application was done on smooth finish steel Q-panels using a BYK drawn down bar at 4 and 8 mil wet film thickness. Panels were then left on the lab bench at ambient conditions to cure. Coatings were tack free after one hour, dry through after one day, and fully cured after three days.

Attenuated Total Reflection Fourier Transform Infrared Spectroscopy

ATR-FTIR was used to characterize the coatings. A Thermo Scientific Nicolet 8700 FT-IR instrument (MA, USA) with Smart iTR™ accessory was used to collect all the spectra in the 4000-400 cm^{-1} range.

Surface Characterization

Water contact angle (WCA) and surface free energy (SFE) were determined using a Kruss® DSA100 drop shape analyzer (Kruss, Germany). Coatings were placed on the stage with no tilt. For each sample five measurements were done where 2μl of water and methyl diiodide (MDI) were dropped onto the sample using a dual-dosing attachment. After the droplets settled, the WCA and MDI measurements were taken and using the Advance^{TM} software, the SFE was determined by the Owens-Wendt calculation.[8]

Ice Adhesion

The procedure for the ice adhesion measurements has been previously published.[20] Ice adhesion measurements were done at -10°C using a Peltier-plate system. Pieces of ice (1 cm x 1 cm x 0.6 cm) were frozen onto the coated substrate and removed using a Nextech DFS500 force gauge at a velocity of 74 μm/s. For critical length measurements, a larger Peltier-plate was used. A Laird Technologies Peltier-plate with length of 22 cm and width of 6 cm was used. For these tests the length of ice was varied from 1 cm to 20 cm while the width and height remained at 1 cm and 0.6 cm respectively. Five measurements were taken for each length of ice.

Biological Assays

Microorganism fouling assays were conducted on eleven sample coatings and five commercial coatings to use as a baseline. Barnacle assays were conducted on nine sample coatings and one commercial coating. Coatings were prepared on aluminum panels that were sandblasted and primed using Intergard 264. 15 mm disks were punched out of the panels and then glued into the base of the Falcon 24-multiwell plates. All wells and panels were pre-leached for 28 days with tap water recirculating every 4 hours. After the 28 days the biological assays were conducted.

-Cell Attachment and Removal of Diatom *(N. incerta)*

First leachate toxicity screening was conducted by immersing the well plates in recirculating water for 7 days. After this time, the plates were incubated for 24 hours in 1.0 ml of Guillard's F/2 growth medium. The extracts were collected, and 1 ml was mixed with 0.05 ml of *N. incerta* along with growth medium. A 0.150 ml aliquot of this solution was transferred to a 96-well plate incubated for 48 hours at 18°C with a 16:8 light:dark cycle. After the incubation, the *N. incerta* biomass was measured by fluorescence intensity of chlorophyll *a* and recorded in relative fluorescence units (RFU). A positive growth control containing nutrient medium, and a negative growth control made from 6 μm of triclosan were used to compare relative toxicity. For biofilm growth, a suspension of *N. incerta* diatoms (~10^5 cells/mL) were diluted to an OD of 0.03 at absorbance 660 nm in artificial seawater (ASW) containing Guillard's F/2 medium. 1 mL of the ASW containing N. incerta was added to each well and then incubated for 48 hours at 18°C with a 16:8 light:dark cycle. After incubation, the biomass was extracted using 1 ml of dimethyl sulfoxide and 0.150 ml of the extracts were again measured for chlorophyll *a* fluorescence and recorded as RFU. The *N. incerta* was given 2 hours to settle on the surface and then water jet removal was done. With three columns for each sample, the first column was not water jetted. The second column was water jetted for 10 seconds at 10 psi. The third column was water jetted at 20 psi. The water jet removal was reported in RFU as biomass remaining, which was measured using chlorophyll *a* fluorescence, and 1-way ANOVA statistical analysis was used to determine the adhesion results.

-Biofilm Growth and Removal of Bacteria *(C. lytica)*

To test the toxicity, the samples were placed in recirculating water with for 7 days. After that they were incubated in 1 ml of biofilm growth medium (BGM) for 24 hours. The extracts

from this were then mixed with 0.05 ml of *C. lytica* (~10^8 cells/mL) and suspended in BGM. A 0.150 ml aliquot of this mixture was then transferred to a 96-well plate and incubated for 24 hours at 28°C. The growth was measured by adding 0.5 ml of 0.35% crystal violet solution. After fifteen minutes, each well was rinsed three times with DI water. Then the crystal violet biofilm was extracted using 0.5 mL of 33% glacial acetic acid. A 0.15 mL aliquot of this extract was transferred to a 96-well plated. Absorbance was measured at 600 nm using a multi-well plate spectrophotometer. A BGM positive growth control and negative growth control (15 μg/mL of triclosan in BGM) were included for reference. For biofilm growth, *C. lytica* was rinsed with 1 ml of ASW and suspended with BGM to a density of ~10^7 cells/ml. Then 1 ml of that solution was added to each well and incubated for 24 hours at 28°C. The plates were tested with the water jet the same as the *N. incerta* except spray time, which was 5 seconds. Biofilm remaining was determined by ATP bioluminescence and was reported as fluorescence intensity. The same statistical analysis was done to determine the adhesion results.

-Attachment and Removal of Barnacles *(A. amphitrite)*

For each sample coating, six adult barnacles were removed from a glass panel which was coated with Silastic-T2 and then immobilized on the surface of the sample coating using a custom template. The barnacles were fed with brine shrimp and left to grow for 2 weeks. After this, the barnacles were removed using a handheld force gauge which measure peak force to detach the barnacle from the surface. After removal, the basal plate area was determined using Sigma Scan Pro 5.0. Barnacle adhesion strength (MPa) was calculated by dividing the force to remove the barnacle by the respective basal plate area. Barnacles that required no force for removal were considered to have not attached to the surface and were recorded as such.

Results and Discussion

One of the main approaches to lower ice adhesion is to modify the surface properties by making the surface hydrophobic. This can be done by utilizing additives or changing surface roughness to obtain a micro/macrostructure. Epoxy-siloxane coatings are a current system used as the topcoats for ship hulls and superstructure. These epoxy-siloxane coatings exhibit high strength and good weatherability, especially UV protection. The goal of this study was to modify the epoxy-siloxane system to improve the surface properties. To do this, siloxane copolymer and homopolymer oils of various composition were integrated into an epoxy-siloxane network to determine the effects of the hydrophobicity of the surface regarding the ice releasing properties. Studying the anti-fouling/fouling release (AF/FR) properties of the coatings were a secondary goal. A base epoxy-siloxane was made based on a published procedure. Once the base coating was successfully made, it was modified with the siloxane oils.

ATR-FTIR was used to characterize the coatings to measure any difference of surface chemistry seen between the various oil compositions used. As seen in Figure 2.1, no significant difference was seen between the coatings. This was not an unexpected result as the oils are added in such a small amount.

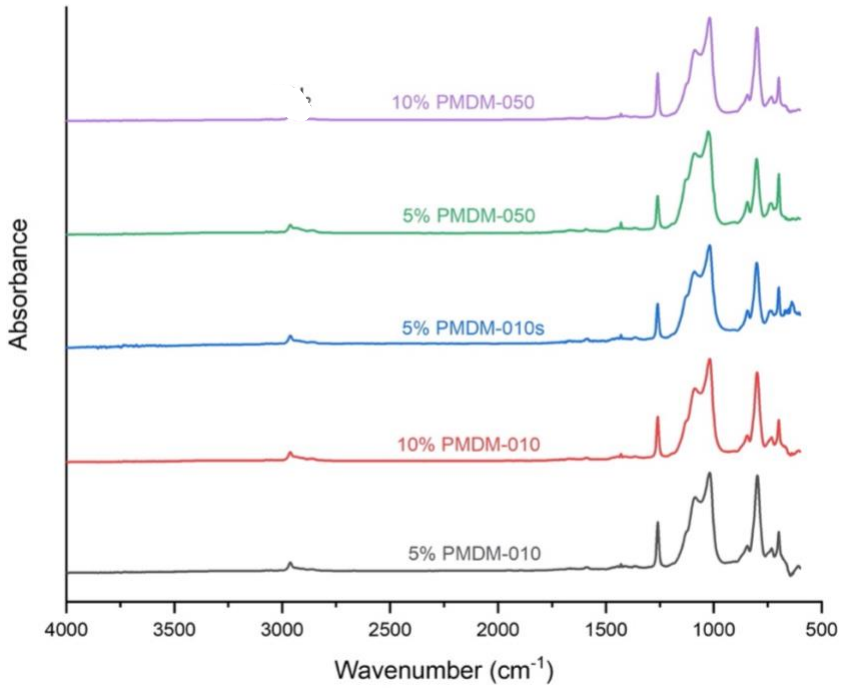

Figure 2.1. ATR-FTIR of methyl and phenyl dominant polysiloxane coatings.

The effects of the oil additives were first measured by determining static water contact angle (WCA). Measurements of the base coating were also done to act as a control. All the measurements were done on a level stage. Five measurements were taken on each coating across the entire length of the panel. In general, the coatings with methyl dominant oil had a higher contact angle and the coatings with phenyl dominant oil had a lower contact angle (Figure 2.2). As the concentration of oil was increased in the coatings this trend became more apparent. As seen in Figure 2.2, the methyl dominant oils had a higher contact angle at 10% vs 5%. Oppositely, the phenyl dominant oils had a lower contact angle at 10% vs 5%. Esumi et al. reported a polydiphenylsiloxane coating with a surface energy of 46.5 mN/m. The coatings with higher percentage of PDMS are yielding a higher contact angle. This makes sense due to the hydrophobicity of PDMS.

The samples that consistently showed a high contact angle were the PMDM-010 coatings. In all the coatings containing this oil, the contact angle was over 100° regardless of

coating thickness, oil concentration, or solvent concentration. In addition to the PMDM-010 coating's high contact angle, these coatings produced the best films. While the DM-100 coatings, which are pure PDMS, had a similar contact angle to the PMDM-010 coatings, the films produced were uneven and rough. On the other hand, the PMDM-050, PMDP-50, and PM-100 coatings yielded a low contact angle slightly above the base coating. The 10% PMDP-050 and 10% PM-100 formulations, containing oils with high phenyl content, had a contact angle significantly lower than the base. This result further indicates the hydrophilic effect that the phenyl dominant oils have on the surface properties of this system.

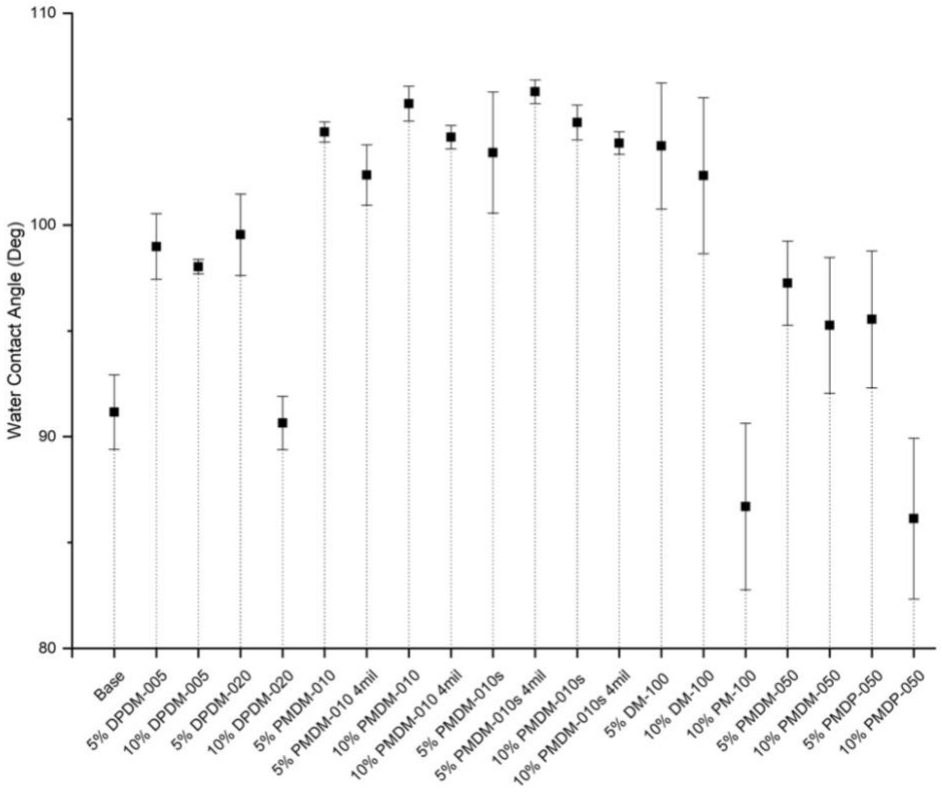

Figure 2.2. Static water contact angle of oil containing coating formulations and the base.

An unexpected result was the higher contact angle seen in the "s" formulations. In nearly all samples with additional solvent, the "s" coating had a higher contact angle compared to its counterpart. Initially the extra solvent was added to improve flow and create a more uniform

film, but the results indicate that this extra solvent is affecting the surface properties in some way. One thought for this is the extra solvent creates more mobility in the system, which allows more silicone oil to get to the surface before the coating cures.

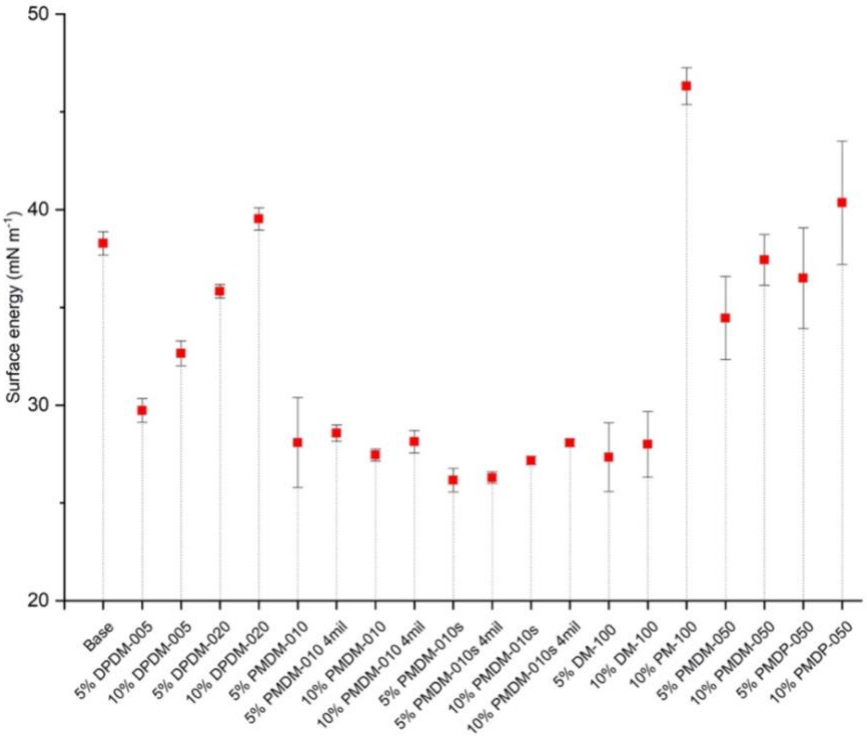

Figure 2.3. Surface energy of oil containing coating formulations and the base.

Ice adhesion measurements were done by pushing a 1 cm^2 block of ice off the sample and recording the force required to break the ice free. Further measurements including critical length, critical force, and interfacial toughness were determined by freezing pieces of ice of different lengths onto the coatings and recording the force required to detach the ice. The latter approach provided a test more comparable to real world scenarios. When ice accretion occurs on aircraft, wind turbine blades, or ships it forms in large sheets. Understanding how large pieces of ice detach from a surface is important in order to design materials specifically for easy removal of large pieces of ice. Ice adhesion measurements were conducted on several the coatings specifically chosen to monitor potential trends. Coating thickness, solvent concentration, oil

concentration, and oil composition were varied, and ice adhesion was measured to see the effects of these changes on the surface properties of the epoxy-siloxane base coating.

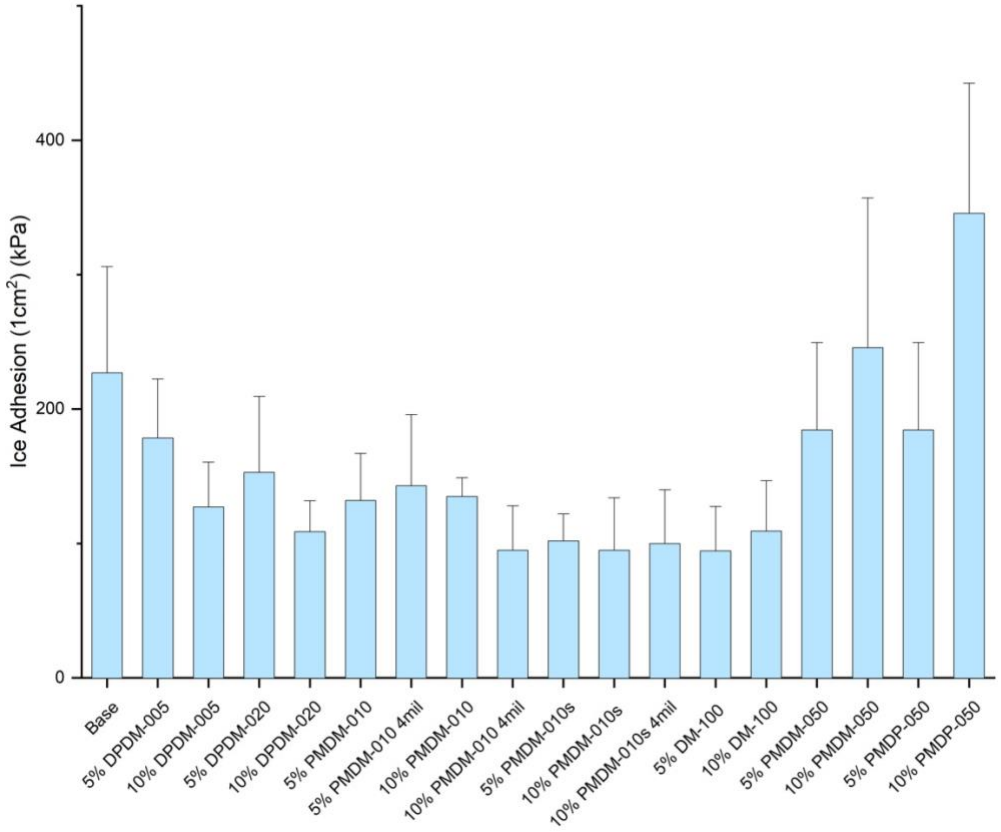

Figure 2.4. Ice adhesion of 1 cm x 1 cm pieces of ice on unmodified and modified epoxy-siloxane coatings.

The trends seen in the contact angle measurements seem to correlate to the ice adhesion results well. The composition of the oil additive had significant influence on the ice adhesion results as it did in the contact angle and surface energy measurements (Figure 2.4). The coatings with methyl dominant oil additive required lower force to detach the ice than the coatings with phenyl dominant oils. Some of the coatings with phenyl dominant oils required much more force to remove the ice than the base coating. Both PMDM-050 and PMDP-050 had a higher ice adhesion than the base coating. The 10% PMDP-050 had the highest ice adhesion at a level much higher than the base coating. Regarding film thickness, there does not seem to be a

noticeable difference in ice adhesion between similar coatings having different film thickness. Some formulations showed higher ice adhesion with a thicker film, and some showed the opposite. Changes in the amount of solvent had significant impacts on the results specifically for the PMDM-010 coatings. This was highlighted in the critical length (Figure 2.5) and interfacial toughness results (Figure 2.6). For smaller pieces of ice, adhesion strength is dependent on the area of the coating/ice interface. As the area of this interface increases, the shear stress required to detach it will continue to increase. Critical length is the point at which the shear stress is no longer dependent on the area of interface. At the critical length the force required to remove a piece of ice plateaus and remains constant. This force is considered the critical force.

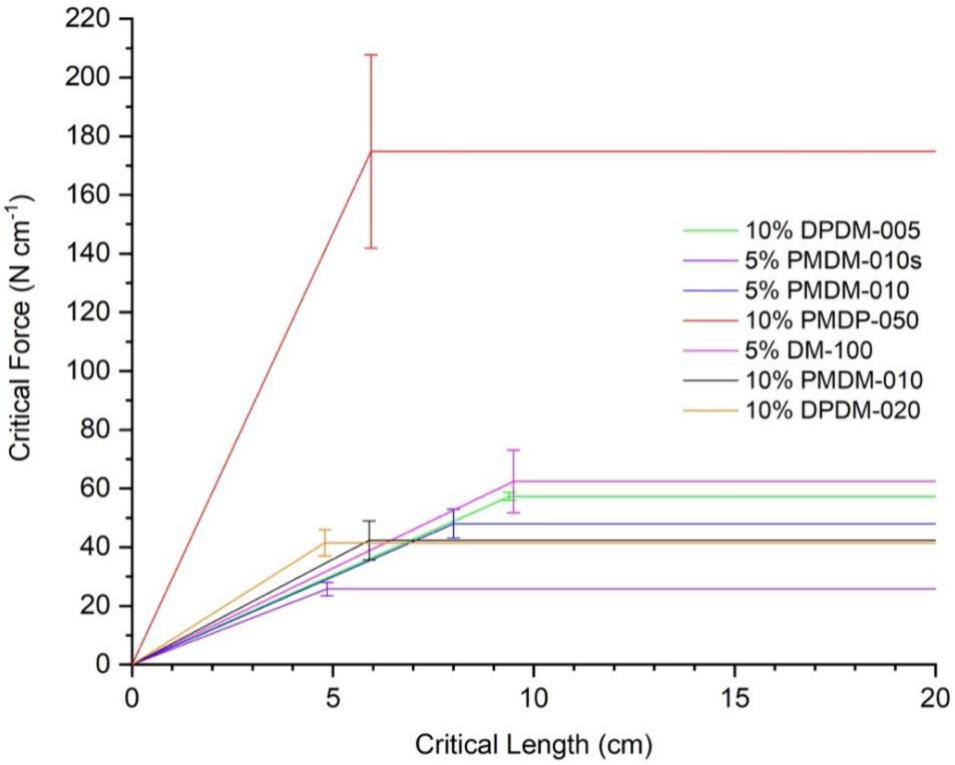

Figure 2.5. Critical force vs critical length of a select group of polysiloxane modified coatings.

Initial ice adhesion results (1 cm^2) showed similar trends to what was seen in the contact angle and surface energy data. The coatings with methyl dominant oil additives performed better than the coatings with phenyl dominant oils, but little difference was seen between the different

coatings with methyl dominant oils. As shown in Figure 2.4, the 10% DPDM-005 and 10% DPDM-020 had a similar low ice adhesion when compared to the 5% PMDM-010s, but when larger pieces of ice were tested the 5% PMDM-010s had the lowest critical force and length out of every other coating (Figure 2.5). The 5% PMDM-010s reached its critical length at approximately 4.85 inches and required the least amount of force to remove long pieces of ice. The 10% DPDM-005 had a similar critical length as the 5% PMDM-010s but required nearly twice the force to remove the ice. An interesting result is the large difference between the 5% PMDM-010 and the 5% PMDM-010s. The only difference between these coatings being more solvent added in the formulation. The critical length of the 5% PMDM-010 is nearly twice the critical length and critical force of the 5% PMDM-010s. Additionally, both the 5% PMDM-010 and 5% PMDM-010s had lower critical length and critical force than the 5% DM-100, which had the highest critical length. This would indicate that the incorporation of some phenyl content into the coating is beneficial to the surface properties of the coatings and may be preferable to pure PDMS. The phenyl dominant 10% PMDP-050 had a slightly higher critical length than the 5% PMDM-010s but a significantly higher critical force than every other coating.

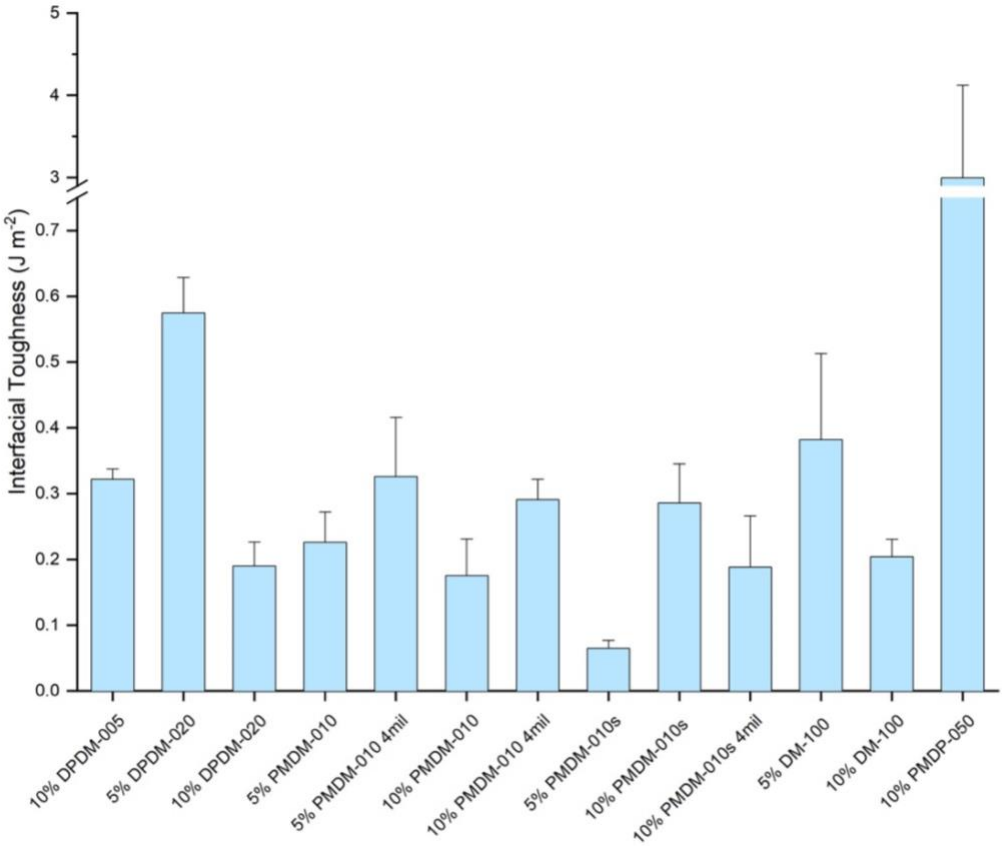

Figure 2.6. Interfacial toughness siloxane oil modified coatings.

The interfacial toughness is calculated using critical force. Interfacial toughness is the resistance an interface has to crack propagation. For large scale deicing, a low interfacial toughness is desirable. This indicates that the force required to remove a large piece of ice is low. The coatings with phenyl dominant oils had higher interfacial toughness than the coatings with methyl dominant oils. The 10% PMDP-050 had an interfacial toughness tenfold the other coatings tested. The 5% PMDM-010s on the other hand, had an interfacial toughness of 0.06 J/m^2, which is lower than the interfacial toughness due to Van der Waals forces (0.1 J/m^2).[9] This result is quite significant, even more so when considering the difference in interfacial toughness seen between the 5% PMDM-010s and the 5% PMDM-010. The additional solvent lowered the interfacial toughness of the coating from 0.23 to 0.06 J/m^2.

The first assay done was using the microalgae *Navicula incerta* (*N. incerta*). First the coatings had to be checked for leachate toxicity. For 28 days water was circulated in tanks containing the coatings. After this, the seawater solution that had been exposed to the coatings was removed and *N. incerta* was grown in this solution. Failure of the *N. incerta* to grow in this solution would indicate that the coating is toxic, which makes the coating unacceptable for use in a marine environment. For these assays, fluorescence is directly proportional to the cells of algae present. To determine the level of toxicity, G+ was used as the positive control indicating a coating that is non-toxic while Tcs is the negative control indicating a highly toxic coating. As seen in the results in (Figure 2.7**)** the solution for all the coatings exhibits no significant level of toxicity as the algae was able to grow similar to the positive control. Figure 2.8 shows the amount *N. incerta* that attached to the surface of the coatings in a two-hour time frame. Then, after two hours, a water jet at 10 psi and 20 psi was used to spray each coating for five seconds and the biomass of *N. incerta* remaining was recorded using fluorescence. Most of the coatings, except the commercial coatings, performed similarly to the others. The sample coatings did not exhibit AF/FR properties as the biofilm was able to attach to the surface of the coatings and was not easily removable. The commercial coatings outperform all the sample coatings with the 1100SR performing the best overall for AF/FR properties.

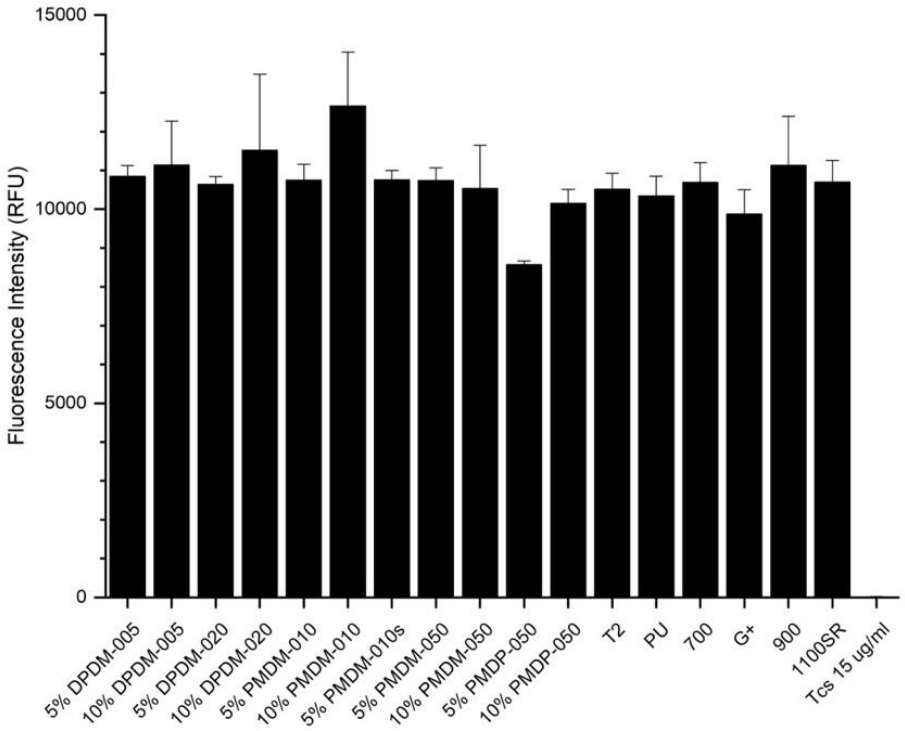

Figure 2.7. *N. incerta* leachate solution toxicity of sample and commercial coatings.

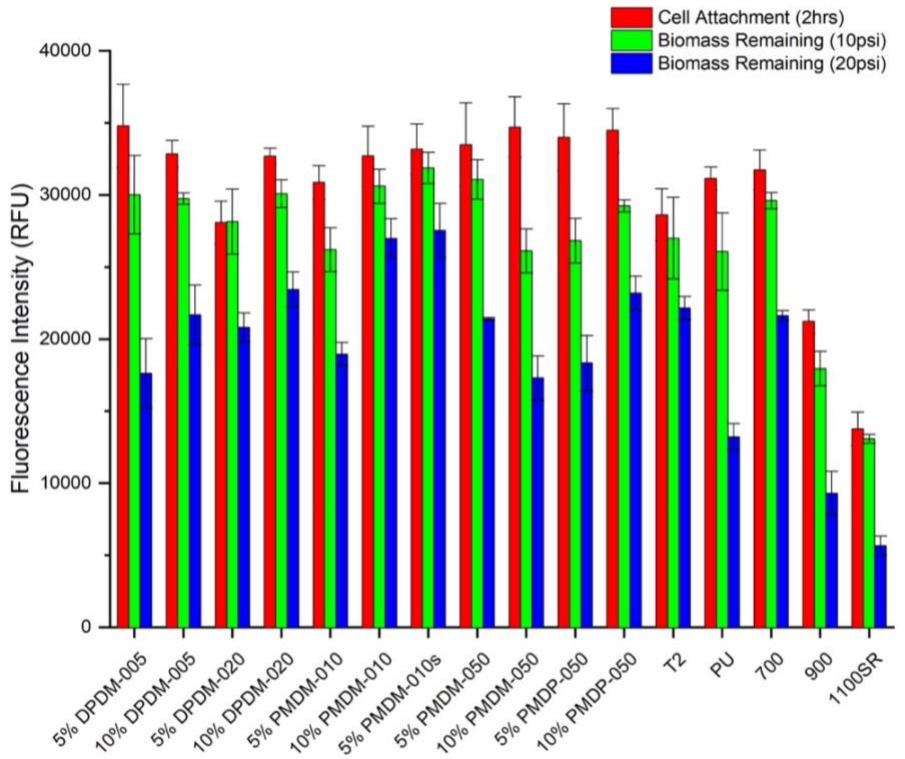

Figure 2.8. *N. incerta* cell attachment and cells remaining after water jet cleaning.

The next assay conducted was with the microorganism *Cellulophaga lytica* (*C. lytica*). Again, leachate toxicity tests were first performed. For *C. lytica* toxicity was tested on the solution as well as on the coating itself (Figure 2.9). Like the first assay performed, the coatings showed no toxicity towards *C. lytica* in the solution or on the coatings. Similar to the *N. incerta*, the samples coatings did not prevent the attachment of *C. lytica* onto the surface, and none of the samples performed better than the others. Overall, the sample coatings had better releasing properties of *C. lytica* compared to the *N. incerta*. Little difference was seen for the removal of *C. lytica* between the 10psi and 20psi water jet. For the *N. incerta* the difference was more significant. Again, sample coatings did not perform as well as the commercial AF/FR coatings (Figure 2.10). The sample coatings performed only slightly better than a plain polyurethane coating. No significant difference was seen between the sample coatings. These results indicate that for microfouling organisms, these coatings do not perform well as AF/FR coatings.

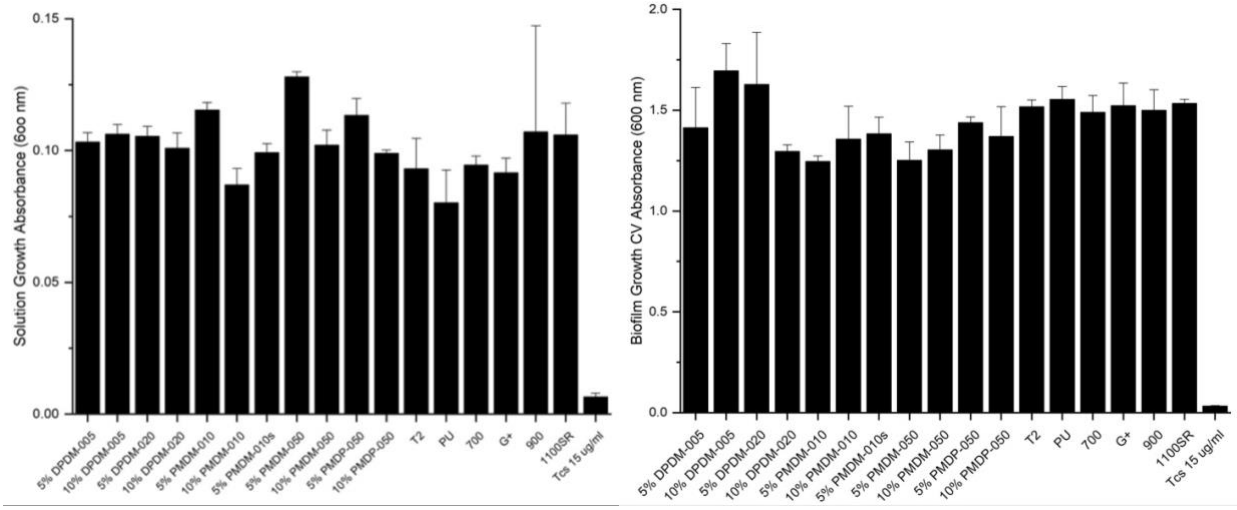

Figure 2.9. *C. lytica* leachate toxicity in solution and on coating surface.

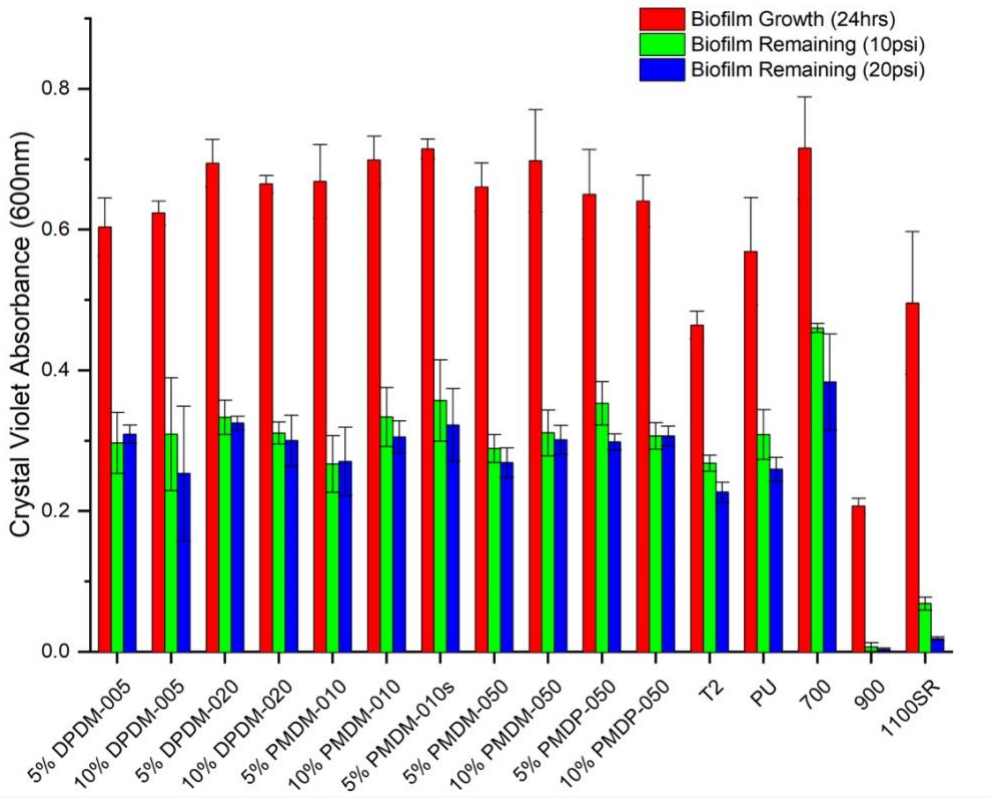

Figure 2.10. *C. lytica* biofilm growth and biofilm remaining after water jet removal.

Lastly, the coatings were exposed to the macrofouling organism *Amphibalanus amphitrite* (barnacles). Barnacle fouling is a significant challenge that is difficult to mitigate due to the barnacle's ability to adhere to many surfaces. Because of the limited availability of live barnacles, only certain coatings could be tested for the barnacle adhesion. The coatings were selected based on ice adhesion performance as well as some phenyl dominant coatings to compare against. In addition to these coatings, three commercial AF/FR coatings were tested. The results can be seen in Figure 2.11 The trends seen in the ice releasing data do not seem to translate to the barnacle adhesion. The PMDM-010 coatings performed well in both, but an interesting result is the low barnacle adhesion force for 10% PMDP-050 considering its low contact angle. While not all the oils that had a high contact angle performed well in the barnacle adhesion, the PMDM-010 coatings did. The higher level of methyl content seems to improve

both contact angle as well as the barnacle adhesion. The 10% PMDM-010 and the 5% PMDM-010s performed similarly with the industry standard Intersleek 1100SR on barnacle removal force.

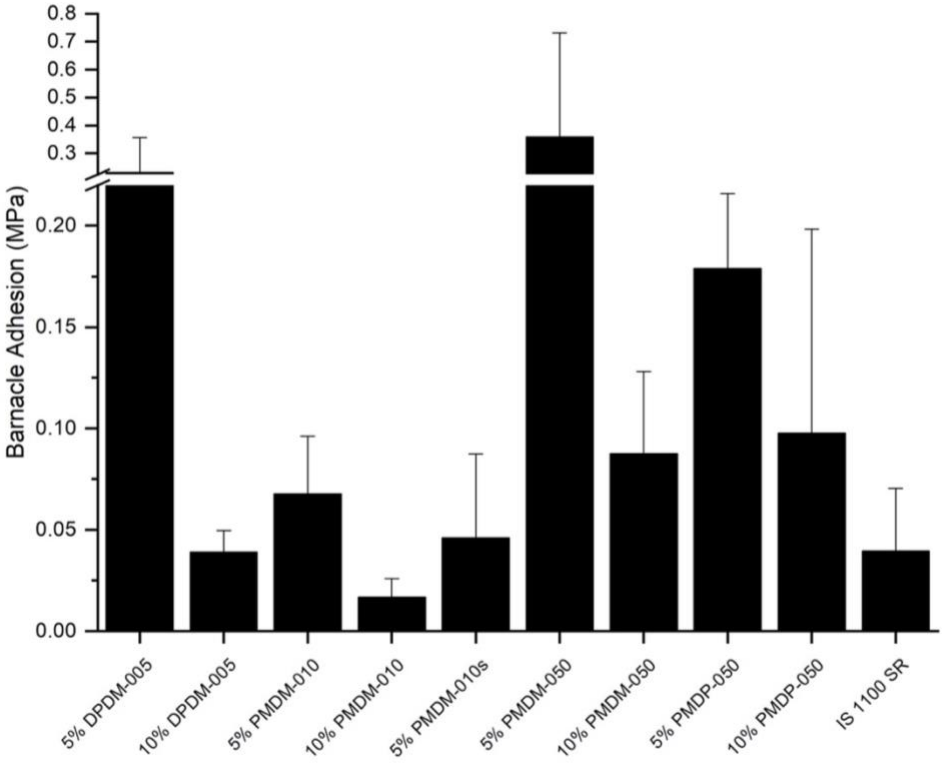

Figure 2.11. Barnacle adhesion of modified epoxy-siloxane coatings and the commercial coating Intersleek 1100SR.

One theory for why the coatings have largely differing surface properties, is the miscibility of the oils in the epoxy-siloxane matrix. The miscibility predictions (Figure 2.12) directly correlate to the contact angle and ice releasing data that was collected. It seems that the coatings with oils that are less miscible in the matrix produce a coating that is more hydrophobic and has exceptional ice releasing properties. Whereas the coatings with oils that are more miscible, produce a coating that is more hydrophilic and has poor ice releasing properties. This would make sense as a less miscible oil will be forced to the surface of the coating where it can

influence the surface properties. The coating with the least miscible oil, PMDM-010, had the lowest ice adhesion and interfacial toughness.

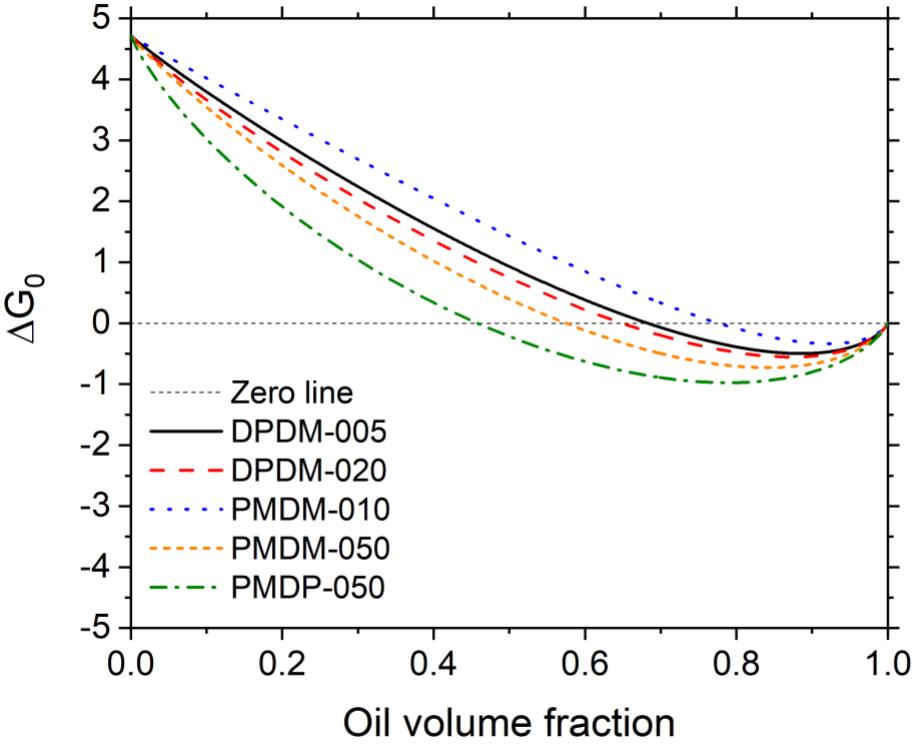

Figure 2.12. Miscibility predictions of silicone oils in epoxy-siloxane matrix.

When looking at the miscibility predictions, even the most miscible oil is not miscible until a volume percent of about 40%. The coatings prepared had much less oil additive than this. The hypothesis is that there is a gradient present near the surface of the coating, and the concentration of the oil in that gradient depends on the miscibility of the oil. The oils that are more miscible will likely be concentrated deeper in the coating, away from the surface where it can influence of the surface properties. The oils that are less miscible will likely be concentrated near the surface of the coating. Visual inspection of the coatings supports this hypothesis, as the more miscible oils produce a clear coating, and the less miscible oils phase separate, producing an opaque coating. Initial miscibility predictions are so far aligning with the experimental data

collected. These predictions do not account for the presence of solvent or what happens while curing, but they could be a useful tool in identifying how other oils may interact with the coating matrix and influence the surface properties. Further testing is necessary to determine if miscibility could potentially be an indicator of surface properties in these coatings

Conclusions

In this study, an epoxy-siloxane coating was successfully prepared. Upon successful preparation of the base, the coatings were modified with additional polysiloxane oil additives. These oils were added with the goal of improving the surface properties of the epoxy-siloxane base, specifically the ice releasing properties. The additives used were a variety of methyl and phenyl siloxane copolymers that were incorporated into the base coating. The modified coatings were then studied to understand the effects that each oil had on surface properties. The surface characterization was conducted with contact angle, surface energy, and ice adhesion tests. One coating formulation performed well in all experiments conducted. Formulation 5% PMDM-010s yielded increased hydrophobicity and lowered ice adhesion. Marine biofouling was tested by performing laboratory assays using two common microorganisms, *Cellulophaga lytica* and *Navicula incerta*, and one macro-organism, *Amphibalanus amphitrite* (barnacles). Biofouling assays were conducted with the intention of drawing comparisons between fouling releasing and ice releasing properties. For microorganisms the sample coatings did not perform as well as the commercial coatings. For barnacles some of the coatings containing methyl dominant oils performed equally to Intersleek 1100SR. The best performing coating was the 5% PMDM-010s. It had the second lowest a low ice adhesion shear strength and very low interfacial toughness, lower than Van der Waals (0.1 J/m^2). The 10% PMDM-010, which also exhibited good ice releasing properties outperformed the Intersleek 1100SR on barnacle adhesion.

References

(1) Mowrer, N. R.; Foscante, R. E.; Rojas, J. L. Epoxy polysiloxane coating and flooring compositions. US 5 618 860, 1997.

(2) Delor-Jestin, F.; Drouin, D.; Cheval, P.-Y.; Lacoste, J. Thermal and photochemical ageing of epoxy resin–Influence of curing agents. *Polymer Degradation and Stability* **2006**, *91* (6), 1247-1255.

(3) Tian, Y.; Yuan, Z.; Huang, X.; Liu, C.; Li, S.; Lu, D. High-efficiency enhancement of the surface weatherability and electrical and mechanical properties of a cycloaliphatic epoxy-based hybrid nanocomposite via reaction-induced organic functional groups. *Progress in Organic Coatings* **2020**, *148*, 105830.

(4) Mehta, P. S.; Mehta, A. S.; Mehta, S. J.; Makhijani, A. B. Bhopal tragedy's health effects: a review of methyl isocyanate toxicity. *Jama* **1990**, *264* (21), 2781-2787.

(5) Valentine, C.; Craig, T.; Hager, S. Inhibition of the discoloration of polyurethane foam caused by ultraviolet light. *Journal of cellular plastics* **1993**, *29* (6), 569-588.

(6) Moravek, S. J.; Rakiewicz, E. F.; Schwartzmiller, D. J.; Zalich, M.; Valenta, J. N. Method of mitigating ice build-up on a substrate. US 8 747 950 B2, 2014.

(7) Kuliasha, C. A.; Fedderwitz, R. L.; Stafslien, S. J.; Finlay, J. A.; Clare, A. S.; Brennan, A. B. Anti-biofouling properties of poly (dimethyl siloxane) with RAFT photopolymerized acrylate/methacrylate surface grafts against model marine organisms. *Biofouling* **2021**, *37* (1), 78-95.

(8) Owens, D. K.; Wendt, R. Estimation of the surface free energy of polymers. *Journal of applied polymer science* **1969**, *13* (8), 1741-1747.

(9) Severin, J.; Hokke, R.; De With, G. Adhesion of electrolessly deposited Ni (P) layers on alumina ceramic. I. Mechanical properties. *Journal of applied physics* **1994**, *75* (7), 3402-3413.

(10) Esumi, K.; Meguro, K.; Schwartz, A. M.; Zettlemoyer, A. C. The Effect of Ultraviolet Radiation on the Wattability of Silicone Polymers. *Bulletin of the Chemical Society of Japan* **1982**, *55* (9), 3019-3020.

(11) Launer, P.; Arkles, B. Infrared analysis of organosilicon compounds: spectra structure correlation silicon compounds. *Gelest Inc: Morrisville, PA* **1987**.

(12) Lejars, M.; Margaillan, A.; Bressy, C. Fouling release coatings: a nontoxic alternative to biocidal antifouling coatings. *Chemical reviews* **2012**, *112* (8), 4347-4390.

(13) Yebra, D. M.; Kiil, S.; Dam-Johansen, K. Antifouling technology—past, present and future steps towards efficient and environmentally friendly antifouling coatings. *Progress in organic coatings* **2004**, *50* (2), 75-104.

(14) Davidson, I. C.; Brown, C. W.; Sytsma, M. D.; Ruiz, G. M. The role of containerships as transfer mechanisms of marine biofouling species. *Biofouling* **2009**, *25* (7), 645-655.

(15) Truby, K.; Wood, C.; Stein, J.; Cella, J.; Carpenter, J.; Kavanagh, C.; Swain, G.; Wiebe, D.; Lapota, D.; Meyer, A. Evaluation of the performance enhancement of silicone biofouling-release coatings by oil incorporation. *Biofouling* **2000**, *15* (1-3), 141-150.

(16) Galhenage, T. P.; Hoffman, D.; Silbert, S. D.; Stafslien, S. J.; Daniels, J.; Miljkovic, T.; Finlay, J. A.; Franco, S. C.; Clare, A. S.; Nedved, B. T. Fouling-release performance of silicone oil-modified siloxane-polyurethane coatings. *ACS applied materials & interfaces* **2016**, *8* (42), 29025-29036.

(17) He, Z.; Zhuo, Y.; Wang, F.; He, J.; Zhang, Z. Design and preparation of icephobic PDMS-based coatings by introducing an aqueous lubricating layer and macro-crack initiators at the ice-substrate interface. *Progress in Organic Coatings* **2020**, *147*, 105737.

(18) Shamshiri, M.; Jafari, R.; Momen, G. Icephobic properties of aqueous self-lubricating coatings containing PEG-PDMS copolymers. *Progress in Organic Coatings* **2021**, *161*, 106466.

(19) Upadhyay, V.; Galhenage, T.; Battocchi, D.; Webster, D. Amphiphilic icephobic coatings. *Progress in Organic Coatings* **2017**, *112*, 191-199.

(20) Golovin, K.; Dhyani, A.; Thouless, M.; Tuteja, A. Low–interfacial toughness materials for effective large-scale deicing. *Science* **2019**, *364* (6438), 371-375.

CHAPTER 3. FUTURE WORK AND CONCLUSIONS

The research in this thesis explored the modification of an epoxy-siloxane coating for the purpose of developing an ice releasing coating. An epoxy-siloxane coating was formulated and then modified using polysiloxane oils. Polysiloxane oils of different composition were incorporated in the epoxy-siloxane to compare the effects that each had on the surface properties. This was done with the intention of discovering trends that could lead to a better understanding of the relationship these siloxane oils have with the surface properties of the material.

Optimization of Epoxy-Siloxane System

The formulation instructions previously published were limited in detail.[1] Example formulations were given with quantities of reagents, but methodology was vague. Instructions like ‘stir until uniform’ were used throughout the publication. Specific processes and stirring times were not provided, so the methods for this study were decided on and then kept consistent. In addition to the vague instructions, there were other formulation examples presented in the publication that were not prepared or tested in this study. The focus of this research was studying the effects of the oil additives on the surface properties and ice adhesion. There is much research that could be conducted to optimize the base coating. A study focused on the base coating could be conducted looking at parameters such as stir time, reagents, reagent quantities, sweat in times, etc. The optimization of the base coating could provide further insight into ways to improve mechanical properties of the overall material.

These same concepts could be explored regarding the modified coatings as well. Again, with no detailed formulation process, there is potential for optimization of these coatings. The incompatibility of the siloxane oils in the epoxy-siloxane matrix is key to the final surface properties. The presence of silicone oil at the surface creates a slippery lubrication layer that

limits ice adhesion. The siloxane oils are being dispersed into the epoxy-siloxane system and then phase separating. It seems that the level of miscibility between the oil and the matrix determines the extent of this phase separation. Stirring time and intensity could change the dispersion of the siloxane oils in the coating. In this study all formulations were stirred for 30 minutes. With a longer stir time, the dispersion of the oil in the epoxy-siloxane could be quite different. The fouling and ice releasing properties of the oils are dependent on the presence of oil domains at the surface. Longer stir times could change the size and distribution of those domains across the surface and could potentially alter the surface properties. This is something worth exploring further. Studying the change in surface properties that arise from varying the stir times, could provide a clearer procedure for optimizing the surface properties of this coating.

Influence of Miscibility on Properties

In this study, solvent quantity significantly affected the ice releasing results, particularly the interfacial toughness. The reason for this is unknown but is believed to be related to miscibility of the oils. Further research could explore the role of solvent in the coating system. The miscibility of the oils in the epoxy-siloxane causes phase separation bringing the oils to the surface. A potential explanation for the improvement of ice releasing properties, is that the additional solvent is affecting the miscibility, or it is affecting the migration of the oils to the surface.

Amphiphilic Oil Additives

Amphiphilic additives are currently used for designing non-toxic fouling release coatings. The additives are a block copolymer of polyethylene glycol (PEG) and PDMS. The current industry standard, Intersleek® 1100SR, is an amphiphilic silicone elastomer. While it is non-toxic and offers impressive AF/FR properties, it suffers from poor mechanical strength, and low

adhesion. This requires the use of a robust base coat, followed by a tie coating for proper adhesion. Further study could involve incorporating an amphiphilic additive, similar to the one found in Intersleek® 1100SR, into the epoxy-siloxane system to explore the fouling and ice releasing properties. Research of these additives has been extensively conducted, specifically studying the effect of composition and structure of the oil additives on the AF/FR properties.[2-4] The typical base coating used was a polyurethane, so it could be valuable to see how these additives perform with the epoxy-siloxane base. Additionally, not much testing has been done to determine the ice releasing properties of coatings modified with these additives.

References

(1) Mowrer, N. R.; Foscante, R. E.; Rojas, J. L. Epoxy polysiloxane coating and flooring compositions. US 5 618 860, 1997.

(2) Bodkhe, R. B.; Thompson, S. E.; Yehle, C.; Cilz, N.; Daniels, J.; Stafslien, S. J.; Callow, M. E.; Callow, J. A.; Webster, D. C. The effect of formulation variables on fouling-release performance of stratified siloxane–polyurethane coatings. Journal of Coatings Technology and Research 2012, 9 (3), 235-249.

(3) Galhenage, T. P.; Webster, D. C.; Moreira, A.; Burgett, R. J.; Stafslien, S. J.; Vanderwal, L.; Finlay, J. A.; Franco, S. C.; Clare, A. S. Poly (ethylene) glycol-modified, amphiphilic, siloxane–polyurethane coatings and their performance as fouling-release surfaces. Journal of Coatings Technology and Research 2017, 14 (2), 307-322.

(4) Galhenage, T. P.; Hoffman, D.; Silbert, S. D.; Stafslien, S. J.; Daniels, J.; Miljkovic, T.; Finlay, J. A.; Franco, S. C.; Clare, A. S.; Nedved, B. T. Fouling-release performance of silicone oil-modified siloxane-polyurethane coatings. *ACS applied materials & interfaces* **2016**, *8* (42), 29025-29036.